1. Report No.	2. Government Accession No.	3. Recipient's Catalog No.
SWUTC/15/600451-00112-1		

4. Title and Subtitle	5. Report Date
Assessment of Vehicle Performance in Harsh Environments Using LSU Driving Simulator and Numerical Simulations	December 2015
	6. Performing Organization Code

7. Author(s)	8. Performing Organization Report No.
Steve C. S. Cai, Sherif Ishak, Jiexuan Hu	Report 600451-00112-1

9. Performing Organization Name and Address	10. Work Unit No. (TRAIS)
Gulf Coast Center for Evacuation and Transportation Resiliency Department of Civil and Environmental Engineering Louisiana State University Baton Rouge, LA 70803	11. Contract or Grant No. DTRT12-G-UTC06

12. Sponsoring Agency Name and Address	13. Type of Report and Period Covered
Southwest Region University Transportation Center Texas A&M Transportation Institute Texas A&M University System College Station, Texas 77843-3135	14. Sponsoring Agency Code

15. Supplementary Notes

Supported by a grant from the U.S. Department of Transportation, University Transportation Centers Program.

16. Abstract

With the economic booming development of coastal areas, the importance of the traffic planning becomes obvious not only in a hurricane evacuation but also in the daily transportation. Vehicle performance on the freeway during harsh environments is critical to the success of the planning process. The present study aims to study the effect of harsh environments on the driving behavior and vehicle performance. The driving simulator installed in Louisiana State University was used to investigate the driver's behavior and vehicle performance in different adverse conditions such as strong crosswinds, wet road surface, and curving. Modified parameters of the driving simulator were determined to reproduce the real wind loadings according to the vehicle velocity and wind velocity, through the manipulation of appropriate software. While the vehicle performance was recorded in terms of lane offset, vehicle velocity, and heading error, the driver's reaction was measured in the form of the reaction time, steering angle, and the time of pressing on brake and gas pedal, respectively. The results illustrate that a higher wind speed leads to more variance of lane offset and heading error. The rainy weather/wet road surface does have an effect on the vehicle velocity in a strong wind environment. The findings of this study demonstrate the valuable use of a driving simulator to represent different hazardous driving conditions and to develop a statistic model to predict and estimate the driver's behavior and vehicle performance.

17. Key Words	18. Distribution Statement
Wind Forces, CFD, Vehicle Performance, Driving Behavior, Driving Simulator	No restrictions. This document is available to the public through NTIS: National Technical Information Service 5285 Port Royal Road Springfield, Virginia 22161

19. Security Classif.(of this report)	20. Security Classif.(of this page)	21. No. of Pages	22. Price
Unclassified	Unclassified	68	

Assessment of Vehicle Performance in Harsh Environments Using LSU Driving Simulator and Numerical Simulations

By

Steve C. S. Cai, Ph.D., PE

Sherif Ishak, Ph.D., PE

Jiexuan Hu, Research Assistant

Report Number SWUTC/15/600451-00112-1

Study Title: Assessment of Vehicle Performance in Harsh Environments Using Driving Simulator and Numerical Simulations

Performed by:

Southwest Region University Transportation Center
Gulf Coast Center for Evacuation and Transportation Resiliency
Department of Civil and Environmental Engineering
Louisiana State University
3505B Patrick F. Taylor Hall
Baton Rouge, LA 70803

December 2015

EXECUTIVE SUMMARY

With the economic booming development of coastal areas, the importance of traffic planning becomes obvious not only in a hurricane evacuation but also in the daily transportation. Vehicle performance on the freeway during harsh environments is critical to the success of the planning process. On the other hand, large trucks are vulnerable under strong wind due to the large wind forces caused by their large size shapes. Adverse driving environments and roadway conditions have been blamed for many single vehicle accidents, and a series of bad collisions resulted from roadway offset and large heading error. Thus, it is important to understand the performance of both the vehicle and driver behavior in hazardous driving environments.

The present study aims to investigate the safety of vehicles during normal operations as well as emergencies through experimentally and numerically replicating the natural environments. An attempt has been made to obtain the wind forces of the vehicles and simulate the complicated weather, road surface, and driver operational process.

Aiming on the investigation of the vehicle's performance and the driver's reaction when driving through strong crosswind areas, the authors have studied the wind forces acting on the moving vehicle by the computational fluid dynamic (CFD) method and conducted driving simulator tests using the driving simulator installed in Louisiana State University. Firstly, a sedan type vehicle was chosen as the discussing vehicle type and its parameters such as its geometry dimensions and its weight were also studied. Secondly, the numerical simulations of the flow field around the vehicle were carried out, and the wind forces on the vehicle were predicted. Finally, the LSU driving simulator was used to investigate the driver's behavior and vehicle performance in different adverse conditions such as strong crosswinds and wet road surface.

The CFD method was adopted to investigate the crosswind forces on the moving vehicle; in addition, the application of a sliding mesh technology realized the relative motion between the vehicle and the road surface. Compared with the resultant wind method, the sliding mesh technology pushed the vehicle moving forward rather than kept the vehicle static at all times, which mimics the vehicle motion more realistically. Thus, by using the CFD sliding mesh method, the wind forces of the vehicle were closer to the true values.

Modified parameters of a driving simulator were determined to reproduce the real wind loadings in according to the vehicle velocity and wind velocity, through manipulation of appropriate

software. Different harsh environments were built through creating data control files; these environments included scenarios in which the vehicle drove through different types of strong crosswinds in different weather such as clear and rainy weather. While the vehicle performance was recorded as the variables of lane offset, vehicle velocity, and heading error, the driver's reaction was measured in the form of the reaction time and steering angle. Two drivers were recruited for two different wind type conditions, and each driver took tests for ten days in which he/she drove in assigned scenario for one time every day.

Based on the results of the numerical simulations, wind forces on the sedan were determined as well as the vehicle performance and driver's behavior. The following are some highlights from the discussion conducted in this study.

- The numerical simulation using the CFD method is an efficient way of investigating wind forces/aerodynamic coefficients of vehicles. In addition, sliding mesh technology is a good choice to help simulate the relative motion between the vehicle and the road surface.
- Vehicle's motion affects the aerodynamic coefficients of the vehicle, and the aerodynamic coefficients can be expressed as functions of the yaw angle between the vehicle direction and the wind direction.
- The simulator can model different weather scenarios including strong crosswinds and the rainy weather, in which the wind forces on the vehicle are the real time wind effects associated with the vehicle velocity and the wind velocity.
- A higher wind speed leads to a larger mean lateral displacement when crosswinds first hit the vehicle as well as a larger lane offset during the crosswinds attacking time.
- The vehicle performance such as lane offset, steering angle, and vehicle velocity are significantly different (P-value<0.0001) between driving environments and driving days.
- Vehicle plays no obvious different (P-value>0.0001) performance on dry road surface and wet road surface excluding the wind action in this study.
- Drivers' reaction times are influenced by the rain falling insignificant.

The present study has demonstrated a feasible approach to study the driver and vehicle behavior, which, through a future more comprehensive study, may provide a useful basis for traffic designs on highways with complicated topographic and weather conditions and optimization of evacuation routes and strategy that may in turn lead to minimized single-vehicle accident risks.

DISCLAIMER

The contents of this report reflect the views of the author, who is responsible for the facts and the accuracy of the information presented herein. This document is disseminated under the sponsorship of the Department of Transportation, University Transportation Centers Program in the interest of information exchange. The U.S. Government assumes no liability for the contents or use thereof.

ACKNOWLEDGEMENT

The author recognizes that support for this dissertation was provided by a grant from the U.S. Department of Transportation, University Transportation Centers Program to the Southwest Region University Transportation Center.

TABLE OF CONTENTS

LIST OF FIGURES

LIST OF TABLES

1. INTRODUCTION

As a significant part of disasters, vehicle accidents are causing more injuries and casualties than any other natural or man-made disasters in the United States as well as other developed countries. Negative effects of hazardous driving environments on vehicle performance have been recognized worldwide. Large trucks are vulnerable under strong wind due to the large wind forces caused by their large size shapes. Adverse driving environments and roadway conditions have been blamed for single vehicle accidents, and a series of bad collisions resulted from roadway offsets and large heading errors (NHTSA 2008; Liu and Subramanian 2009). In coastal areas, hazardous driving environments may mainly include strong wind and heavy raining weather that also influence the roadway surface conditions. In the United States, according to USDOT, single vehicle fatal crashes and inclement weather induced fatal crashes were responsible for around 22% and 12% of the fatal crashes involving large trucks in 2013, respectively. Large truck accidents threaten people's lives directly. In 2013, there were 3541 fatal crashes and 69,000 injury crashes involving large trucks; in these crashes, 3964 persons were killed, and 95,000 persons were injured (USDOT 2015). Non-collision single vehicle crashes, such as running off the road, losing control of the vehicle, and rolling of the vehicle, have been reported for some time worldwide. Unlike traffic collisions which may cause millions of deaths every year, non-collision single vehicle accidents still have high potential to hurt or kill the driver, riders, and even pedestrians or bicyclists. On the other hand, large truck crashes also cause severe congestion and affect the normal work of the roadway as well as emergency situations, which may lead to serious property damage and economic loss. Non-collision accidents also put many people in miserable situations when an emergency evacuation is interrupted by accidents on key routes. As a result, the safety of many people who are stuck in the evacuation routes may be jeopardized.

For coastal states such as Florida, Louisiana, Mississippi, and Alabama that experience tropical storms frequently, a healthy transportation system exerts a significant positive effect on storm landfall days. The huge number of residents under evacuation order also requires a smooth transportation. Data provided by the Federal Emergency Management Agency (FEMA) indicates that during Katrina, over 1.2 million people along the northern Gulf coast from southeastern Louisiana to Alabama were under some type of evacuation order (Knabb et al. 2005). Thus, the transportation systems, including bridges and highways, have to be kept free for the material

supply of tropical storm areas and evacuation of suffering people. Reducing the occurrence of the vehicle accidents under the storm weather (e.g. strong wind and heavy rain) has become apparent.

The cause of single-vehicle accidents can be very complicated: from a single primary reason such as a strong gust to the combination of several reasons such as weather conditions, vehicle conditions, road surface conditions, driver operational errors, etc. Thus, it is important to understand the performance of vehicles and driver behavior in hazardous driving environments. As an important category of vehicle accidents, single-vehicle non-collision accidents under adverse environmental and topographic conditions have not been studied sufficiently. The present study aims to demonstrate the feasibility of investigating the safety of vehicles during normal operations as well as emergencies through experimentally and numerically replicating the natural environments. An attempt was made to simulate the airflow field around the vehicle when subjected strong winds and obtain the wind forces of the vehicle driving through cross the winds. Based on the wind loads of the vehicle, driving simulator experiments were conducted to test both the vehicle performance and the driver's reaction in adverse weather, such as strong winds and rain. This work may help understand and develop a single vehicle accident assessment framework in which accident risks will be assessed for vehicles.

2. BACKGROUND

This section is presenting some literature reviews of the effects of harsh weather on road vehicles and is divided into four parts: the first part presents an overview of wind forces on vehicles experienced during hurricanes and tropical storms; the second part reviews the simulation of aerodynamic forces of vehicles under cross winds; the third part highlights the studies on the effects of weather on driver behavior, and the fourth part demonstrates the overview of the LSU simulator that was used in this study.

2.1 Wind hazard, tropical storm and hurricane

Wind is air movement relative to the earth surface, driven by multiple forces: pressure differences in the atmosphere due to the differences of solar heating in different parts of the earth and the forces induced by the rotation of the earth. Strong local air convective effects and the uplift air masses also may produce local severe winds. On almost every day of the year windstorms occur on earth, though many storms are small and localized. The high frequency of windstorms brings huge damage to modern structures over a long time period, which is almost equal to the amount of damage produced by the earthquakes that have tended to happen less often than severe windstorms (Holmes 2001). The major windstorms are usually classified as follows:

Thunderstorm: Thunderstorms are small disturbances in horizontal extent and are capable of generating severe winds. Usually, high humidity of lower levels air, instable factors in the atmosphere, and lifting mechanism promoting the initial rapid convection of the air are necessary in the generation of severe thunderstorms. The production of the thunderstorms comprises heavily of rain or hail and strong wind for a short period of time that contribute significantly to the strong gusts recorded in many countries, including the United States, Australia, and South Africa (Holmes 2001; Simiu and Scanlan 1996).

Tornadoes: These are larger and last longer than “ordinary” convection cells. The tornado, a vertical, funnel-shaped vortex created in thunderclouds, is the most destructive of windstorms. They are quite small in their horizontal extent of the order of 100 m. However, they can travel for quite a long distance, up to 50 km, before dissipating, producing a long narrow path of destruction. They occur mainly in large continental plains, and they have very rarely passed over a weather recording station because of their small size (Holmes 2001).

Downbursts: Downbursts have a short duration and also a rapid change of wind direction during their passage across the measurement station. The horizontal wind speed in a thunderstorm downburst, with respect to the moving storm, is similar to that of a jet of fluid impinging on a plain surface (Holmes 2001).

Tropical cyclones: Tropical cyclones are defined as a rotating, organized system of clouds that usually occur over the tropical oceans. Tropical cyclones are developed when water evaporates from the ocean and releases as the saturated air rises, resulting in condensation of water vapor contained in the moist air. The term "tropical cyclones" proclaims their cyclonic nature and the geographical origins, in latitudes from 10 to about 30 degrees, both north and south of the Equator (Holmes 2001).

Tropical cyclones become strengthened over warm water and lose their power if they move over land due to the increase of surface friction and loss of energy source. That is the reason why coastal regions suffer more destructive damage than that of inland regions (United States Department of Commerce 2012). As the most severe one of all wind events, the influence of tropical cyclones can be devastating when these storms make landfall on populated coastlines. Tropical cyclones produce extremely powerful wind and torrential rain as well as high waves, damaging storm surge and tornadoes sometimes.

Tropical cyclones are called different names around the world. They are named hurricanes in the Caribbean, typhoons in the South China Sea, and cyclones in Australia (Holmes 2001). A tropical storm is defined as a tropical cyclone with a maximum sustained wind between 18 to 32 m/s (39 to 73 mph), and a hurricane is tropical cyclone with maximum sustained winds of at least 33 m/s (74 mph) (NOAA 2013, Rodriguez 2014). The wind speeds are estimated at the standard meteorological height of 10 m or 33 ft. The National Hurricane Center (NHC) uses a 1-min averaging time for reporting the sustained winds while The National Weather Service (NWS) adopts a 2-min averaging wind for its sustained wind definition. There is no conversion factor to change a 2-min average wind into a 1-min averaging wind because they are essentially the same (Powell et al. 1996, Rodriguez 2014). For all tropical cyclones, the wind is highly gusty or turbulent. A wind gust is a sudden, brief increase in speed of the sustained wind. It is defined as having a few seconds long (3 to 20 seconds) wind peak. Typically in a hurricane environment, the value of the maximum 3-second gust over a 1-min average is on the order of 1.3 times (30% higher) than the 1-min sustained wind (Powell et al. 1996, Rodriguez 2014).

In 1973, Herbert Saffir and Robert Simpson introduced a hurricane wind scale to the general public. The scale was divided into 5 classifications based on 1-min sustained wind speed and was used to indicate the potential damage and the effects of storm surge and flooding. After several modifications by the NHC, the Saffir-Simpson Hurricane Wind Scale (SSHWS) has the final form as shown in Table 1 (Rodriguez 2014).

Table 1 Saffir-Simpson Hurricane Wind Scale (SSHWS)

Category	1-min sustained winds	Types of damage
1	74-95 mph 64-82 knots 119-153 km/h 33-42 m/s	Very dangerous winds will produce some damage: well-constructed frame homes could have damage to roof, shingles, and vinyl siding and gutters. Large branches of trees will snap and shallowly rooted trees may be toppled. Extensive damage to poles lines and poles likely will result in power outage that could last a few days
2	96-110 mph 83-95 knots 154-177 km/h 43-49 m/s	Extremely dangerous winds will cause extensive damage: well-constructed frame house could sustain major roof and siding damage. Many shallowly rooted trees will be snapped or uprooted and block numerous roads. Near-total power loss is expected with outages that could last from several days to weeks.
3	111-129 mph 96-112 knots 178-208 km/h 50-58 m/s	Devastating damage will occur: well-built frame homes may incur major damage or removal of roof decking and gables ends. Many trees will be snapped or uprooted, blocking numerous roads. Electricity and water will be unavailable for a few days to weeks.
4	130-156 mph 113-136 knots 209-251 km/h 59-69 m/s	Catastrophic damage will occur: will-built frame homes can sustain severe damage with loss of most of the roof structure and/or some exterior walls. Most trees will be snapped or uprooted and power poles downed. Fallen trees and power poles will isolate residential areas. Power outage will last weeks to months. Most of the area will be uninhabitable for weeks or months.
5	157 mph or higher 137 knots or higher 252 km/h or higher 70 m/s or higher	Catastrophic damage will occur: a high percentage of framed homes will be destroyed, with total roof failure and wall collapse. Fallen trees and power poles will isolate residential areas. Power outage will last for weeks to possibly months. Most of the area will be uninhabitable for weeks or months.

The scale can be used to describe the effects of hurricane and predictthe damage and the impacts associated with winds in the United States (Pielke 2008, Rodriguez 2014). Location plays an important role in this scale, for example, a Category 2 hurricane which hits a major city will likely do far more cumulative damage than a Category 5 hurricane that hits a rural area. On the other hand, once a hurricane makes landfall, its wind speed decreases quickly due to the friction of the earth surface. As the second Pacific hurricane on record to make landfall at Category 5 intensity on October 23, 2015, Patricia degraded into a tropical depression and dissipated soon within 24 hours because of the interaction with the mountainous terrain of

Mexico (Sanchez 2015). The scale does not address the potential for storm surge, rainfall-induced floods, or tornadoes.

Hurricane's return periods are the frequency at which a certain intensity of hurricane can be expected within a given distance of a given location. A return period of 25 years for a hurricane, for example, refers to that on average during the previous 100 years a hurricane passed that location about four times (NOAA 2012, Rodriguez 2014). The coast of Louisiana has a return period of 7 to 14 years for a hurricane with sustained winds of 33 m/s or greater and a return period of 20 to 33 years for hurricane with sustained wind speed of 50 m/s (NOAA 2012, Rodriguez 2014).

Hurricanes that have stuck the United States have made deep impressions to Americans due to the results of catastrophic property damages. Ranked using a 2010 deflator, Hurricane Katrina, Andrew, and Ikea took the first three places of the list of the costliest mainland United States tropical cyclones between 1990-2010, which were responsible for at least $105 billion, $45 billion, and $27.7 billion of property damage, respectively. In addition, the United States has experienced 11 out of the top 30 costliest tropical cyclones in the last ten hurricane seasons including Katrina and Ike (NOAA 2011). Based on the amount of monetary loss and the times of enormous hazard hurricane, the negative influence of tropical hurricane becomes more and more obvious. In recent years, the booming of coastal areas is attracting huge population, and these people bring with them ever more personal wealth, which may cause the increase of losses. Pielke et al. (2008) addressed the societal factor in shaping trends in damage related to hurricanes and suggested that the losses will be double every 10 years. For a simple example, a hurricane like the Great Miami hitting the United States mainland would leave about $500 billion of property losses as soon as the 2020s.

In addition to the immense property damages of tropical cyclones, the loss of life is also huge. The Galveston Hurricane of 1900 was the deadliest hurricane in the history of the United States, killing at least 8,000 people. The 1928 Okeechobee Hurricane caused at least 2,500 casualties. The total number of death directly attributed to the Katrina is uncertain. However, the most significant number of deaths occurred in New Orleans, which came out around 1,300; besides that, there were 200 fatalities in Mississippi, 6 in Florida and 1 in Georgia. Beyond the United States, the Bhola cyclone of 1970 killed more than 300,000 people (Holland 1993), which

placed this cyclone as the deadliest tropical cyclone on record. In China, Typhoon Nina of 1975 induced a 100-year flood and resulted in nearly 100,000 fatalities (Weyman and Berry 2008).

Tropical cyclones that cause extreme destruction directly are rare and do not need to be particularly strong to cause damage. The tropical storm induced flood, mudslides, and other disasters also lead to catastrophic damages. Tropical Strom Thelma in November 1991 killed thousands in the Philippines, while in 1982 the unnamed tropical depression that eventually became Hurricane Paul killed around 1,000 people in Central America (Gunther et al. 1983). During Hurricane Katrina, thousands of homes and commercial buildings throughout the entire metropolitan area of New Orleans were ruined by flooding while strong winds peeled the roof off of the Louisiana Superdome (Knabb et al. 2005). Hurricane Mitch of 1998 was the deadliest Atlantic hurricane since 1780, and most deaths were reported from flooding and mudslides in Central America (Guiney and Lawrence 1999).

Although significant efforts have been made on developing storm prediction and tracking technologies, the variable nature of tropical weather is still a big problem in learning hurricane influence. On the other hand, the majority of massive population is expected to evacuate under a benign weather before storm landfall rather than in a harsh weather induced by tropical storm. However, not all preparation can be made in a short time prior of the arrival of storm. Data provided by the Federal Emergency Management Agency (FEMA) indicated that during hurricane Katrina, over 1.2 million people along the northern Gulf coast from southeastern Louisiana to Alabama were under some type of evacuation order, but it was not clear how many actually evacuated (Knabb et al. 2005, Rodriguez 2014).

The high potential risk of suffering tropical storms may hinder the investment of some coastal areas, but the growth of massive population in these areas is tremendous. The increase of the transportation system capacity in these areas is not with the same pace of population. Thus, a reliable transportation route is the key to maximizing the number of evacuees as well as for post-hurricane rescue efforts and the positive performance of transportation (bridge, highway and vehicles) under a windy weather plays an important role in hazard mitigation plan.

2.2 Aerodynamic forces of vehicle

For vehicles driven on highways, the wind loading on the vehicle, along with the grade and curvature of the road, may cause safety and comforting problems (Baker 1991a; Baker

1991b; Baker 1991c; Baker 1994). To more accurately predict the associated accident risks in strong wind, appropriate data is required to quantify the aerodynamic forces and moment coefficients for different types of vehicles (Baker 1986a). In the automobile industry, the research on vehicle aerodynamic performance is mainly focused on reducing the drag force of the vehicle in order to conserve fuel consumption (Malviya et al. 2009; Patten et al. 2012), or on understanding the flow field around vehicles moving on the ground (Angelis et al. 1996; Guilmineau 2008; Corin et al. 2008).

When a vehicle is subjected to crosswind, or overtaking other vehicles, the flow field around the vehicle becomes asymmetric, which is very different from the drag force investigations in the automobile industry. In such a case, the resultant aerodynamic forces have six components that include the side force, yawing moment, and rolling moment in addition to drag force, lift force and pitching moment (Hucho 1993). As the drag force influences the velocity of the vehicle, the side force and yawing moment may cause vehicle instability and handling difficulties. Baker and his co-workers (Coleman and Baker 1990) conducted a series of tests on the vehicle aerodynamic forces and moments under different yaw angles and found that the stream turbulence has significant effect on the lift force, which significantly increases the accident risk. To study the effect of atmospheric turbulence or train and ground relative motion, a catapulted setup experiment was carried out in an atmospheric boundary layer wind tunnel (Baker 1986b), and different types of vehicles (e.g. high side road vehicle, car and small vans), wind speeds and flow fields were studied as the influence factors on the wind load coefficients of vehicles (Baker 1991a, Baker 1991b, Baker 1991c, Humphreys and Baker 1992). The aerodynamic force coefficients of vehicles were found to vary with the vehicle's motion state, the vehicle position relative to others, and the terrain characteristics (Baker 1986b). To investigate the gust effect on ground vehicles, a special testing track was designed and constructed to measure the transient load on the vehicle passing through the gust wind with various resultant yaw angles (Cairns 1994) and it was found that the effect of turbulence is fairly obvious at high yaw angles (Cheli et al. 2011b). A numerical simulation of unsteady crosswind aerodynamics considering the wind-gust boundary layer profiles illustrated that the force coefficients showed highly transient behavior under gusty conditions (Favre 2011).

To investigate the relationship between the wind speed, truck speed, and propensity for truck rollover, Bettle et al. (2003) adopted the CFD method and obtained the aerodynamic forces

acting on a truck travelling through a bridge under cross-wind. The results showed that the vehicle with higher speed was suffering a larger aerodynamic moment that tends to overturn a vehicle in the windward lane of the bridge. The corresponding moments were considerably less for the vehicle in the leeward lane. However, the traveling situation was simulated with fixed vehicles subjected to a resultant wind velocity of the wind velocity and vehicle speed. To investigate the aerodynamic forces on a moving vehicle, Krajnovic and Davidson (2005a) used the resultant wind velocity method in CFD and assigned the ground a moving velocity relative to the fixed vehicle to simulate the vehicle moving on the ground. Corin et al. (2008) simulated the transient aerodynamic forces on overtaking road vehicle models by using the two-dimensional (2D) CFD method. In the study, moving mesh was used to produce the relative motion (overtaking) between two road vehicles. Later, more situations were considered, such as the different supporting infrastructure scenarios, the position of vehicles mounted on the bridge, and the vehicle geometry (Cheli et al. 2011a). Osth and Krajnovic (2012) investigated the flow field around the vehicle body and demonstrated the influence of leading edge shape and gap width between the cab and trailer on the drag force of a simplified tractor-trailer model through the CFD method. As a cross check with the experimental measurements, Han et al. (2013) predicted the aerodynamic force coefficients of vehicles on bridges using a commercial CFD solver ANSYS CFX 12 on a three-dimensional computational model of the vehicle on the section of the bridge. The Shear Stress Transport (SST k-ω) turbulence model is applied to represent the turbulence of the flow. The turbulence model is designed to deal with the adverse pressure gradients, separated flows, and the results show good performance. A reasonable agreement was observed between the experimental and numerical results. By using the similar method to the moving ground case, Wang et al. (2013) studied the aerodynamic coefficients of a moving vehicle-bridge system and evaluated the moving effects on the aerodynamic characteristic of the vehicle and the bridge.

In comparison with the applications of the RAN models as discussed above, Krajnovic and Davidson (2002, 2003, 2005b, and 2005c) have conducted a series of investigations of flow around bluff bodies such as trains, buses, and ground vehicles by using the Large-Eddy Simulation (LES) model to simulate the flow turbulence, in which the LES results showed good agreement with the experimental data. In addition to the vehicles on highways, aerodynamic behavior of trains to crosswind was also investigated by means of CFD methods and wind tunnel

tests (Cheli et al. 2010). Through using LES, Krajnovic et al. (2011, 2012) investigated the flow around a simplified train moving through a crosswind flow. Guilmineau et al. (2013) studied the effects on a simplified car model by a Detached Eddy Simulation (DES) approach. However, in these studies, DES and LES are used in predicting the aerodynamic forces of the vehicle on the ground rather than the vehicle on bridges. Osth and Krajnovic (2014) studied the aerodynamics of a generic container freight wagon using LES.

2.3 Effect of inclement weather on vehicle performance

Inclement weather can influence the freeway capacity as well as the operating speed. Ibrahim and Hall (1994) studied the effects of rain and snow on freeway operations in Canada and tested the inclement weather on the relationship between speed and occupancy. While light rains were reported to cause a vehicle speed drop of 2 km/h and heavy rains reduced about 10 km/m of vehicle speed, light snow and heavy snow induced 2 km/h and 38 to 50 km/h vehicle speed falling, respectively. May (1998) suggested free-flow speeds for different weather conditions that were included in the 2000 version of the Highway Capacity Manual. In clear and dry weather, the recommended value of the free-flow speed was 120 km/h; in light rain and light snow condition, the value should be 110km/h; in heavy rain and heavy snow weather, the speed becomes 100 km/h and 70 km/h, respectively. Oh et al. (2002) studied the speed-flow and the flow-occupancy relationship based field data from two bridges and pointed out that the ratios of free flow speed reduction were observed 7% and 2% by snowy and rainy day time, respectively. Meanwhile, the ratios of speed reduction were 5% and 6% in snowy and rainy night, respectively.

Kyte et al. (2001) reported the effects of visibility, road surface, precipitation, and wind speed on free-flow speed based on the field sensor data in two winter periods. The mean speed of passenger cars was 117 km/h, and the mean truck speed was 98.8 km/h in a normal condition that was without rain, dry road surface, and visibility greater than 0.37 km, and wind speed less than 16 km/h. For the mean speed of all vehicles, it was 109 km/h in a normal condition while a speed drop occurred in rainy weather. The vehicle speed dropped about 14-19.5 km/h and 31.6 km/h in light rain and heavy rain, respectively.

There is a summary of freeway traffic flow reductions due to weather on FHWA's road weather management program website (FHWA 2013). As shown in Table 2, on a freeway, the

impact of rainy weather showed that light rain reduces speed by approximately 10%; heavy rain decreases speed by approximately 16%.

Table 2 Freeway traffic flow reductions due to weather

Weather conditions	Freeway traffic flow reductions			
	Average speed	Free-flow speed	Volume	Capacity
Light rain/snow	3%-13%	2%-13%	5%-10%	4%-11%
Heavy rain	3%-16%	6%-17%	14%	10%-30%
Heavy snow	5%-40%	5%-64%	30%-44%	12%-27%
Low visibility	10%-12%			12%

Besides the speed reduction of weather impacts on transportation, accidents induced by inclement weather also are stunning, especially in a rainy day. Researchers agreed with the factors of skidding accidents, and the factors were dedicated into three categories: drivers' behavior, roadway conditions and environment, and vehicle and its characteristics (Corsello 1993). The way to quantify how easily the vehicle will slip is with the coefficient of friction. The friction force is defined as the tangential resisting force at the tire-pavement interface when braking forces are applied to the tire and the sliding occurs.

The friction force at tire-pavement interface is influenced by many factors, including vehicle features, tire factors, and road surface conditions (Henry, 2000; Hall, et al, 2006). Thus, the friction performance is usually determined by experimental tests. The Washington State Department of Transportation (WSDOT) determined wet-pavement friction characteristics by conducting skid-tests in accordance with applicable AASHTO and ASTM standards. The results of the skid-tests are used in conjunction with other criteria to assist in selecting pavements for resurfacing.

Besides the experimental method, the numerical simulation method was widely applied. Ray (1997) estimated the tire force and identified road friction by both simulation and experimental methods. The sliding friction coefficient is computed using follow equation: (Wang et al, 2010).

$$\mu = F_h / F_v \quad (1)$$

Where μ is the sliding friction coefficient; F_h is the tangential friction force at the tire-pavement surface; and F_v is the vertical load on tire. A well-known "Magic Formula" proposed by Pacejka (2006) can be used for investigating the relationship between the friction force and slip ratio. The formula is shown as equation 2 and is validated by experimental data obtained under various testing conditions.

$$F(s) = c_1 \sin(c_2 \arctan(c_3 s - c_4(c_3 s - \arctan(c_3 s)))) \quad (2)$$

Where $F(s)$ is the friction force due to cornering;c_1, c_2, c_3, and c_4 are model parameters; and s is the slip.

As an external environment factor, rainy weather results in various abnormal conditions when driving on wet road pavement, and rainfall may affect the friction available from the pavement surface. In other words, the rainfall generates a lubricant layer of water under all parts of the tires, which may cause the vehicle hydroplane on the water surface if the water at the tire-pavement interface is not expelled away through the tire tread timely. Due to the complex mechanics of frictions, wet road surface provides low and variable friction values. For example, a "slick" racing tire with no tread may get a friction coefficient as high as 0.9 on a dry road while the friction coefficient would be down to 0.1 on a wet road as a very dangerous condition. Table 3 shows the different static friction coefficients of pneumatic tires on a wet surface. (Robert Bosh GmbH 1996).

Table 3 Coefficient of static friction for pneumatic tire on various condition road surfaces

Vehicle speed (km/h)	Tire condition	Road condition				
		Dry	Wet Water depth≈0.2mm	Heavy rainfall Water depth≈1mm	Puddles Water depth≈2mm	Ice (Black ice)
50	New	0.85	0.65	0.55	0.5	0.1 and less
50	Worn	1.00	0.50	0.40	0.25	
90	New	0.80	0.60	0.30	0.05	
90	Worn	0.95	0.20	0.10	0.05	
130	New	0.75	0.55	0.20	0.00	
130	Worn	0.90	0.20	0.1	0.00	

2.4 The LSU driving simulator

The fact that the LSU driving simulator provides drivers with a high fidelity virtual driving environment is due to the combination of the full size passenger, image projectors, three

large screens, and the software that generates scenarios and controls vehicle dynamics. The full size car is modeled after a Ford Focus automobile with multiple cameras installed in it; the projector and screens in front of the vehicle work together to demonstrate vivid images of road scenarios; the software like SimVista and SimCreator are used to modify the driving environments and control the vehicle's dynamics (Ishak et al. 2013, Rodriguez 2014).

Figure 1 shows pictures of the driving simulator against a projected virtual environment, and some of its series of computer screens. The first two computers are used to control the simulation, the middle one displays the images that are being captured by the cameras, and the last two are used for data analysis. The simulator comes equipped with automated sensing devices and subsystems that gather data such as engine's RPM (revolutions per minute), heading error, vehicle speed, acceleration, trajectory offset, braking, vehicle position, etc. Also included are digital cameras installed within the vehicle. The video from these cameras is also linked to the application software, SimObserver, and is time-referenced with the sensing data.

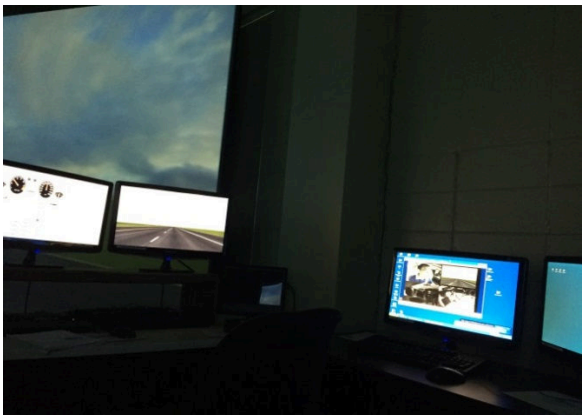

Figure 1 LSU driving simulator system

Figure 2 Still image caputured from video feed

Figure 2 shows a still image captured from the video feed from the four cameras which are located in front and behind of the driver, around foot pedals, and are divided into four windows for the four cameras. The top left corner window shows the video images screened by the front camera in order to capture the driver's facial expression and view direction. The top right window displays the outside views that the driver watches from the vehicle inside. The record of lower left corner exhibits the driver's hand actions captured by the rear camera. The video in the lower right window reflects the foot position of the driver, on brake or on gas. Researchers can use the video to determine a driver's reaction to a stimulant or change and visually verify a driver's behavior during a run. The driving tests can be changed based on

weather conditions, roadway surfaces, and environment by the application software Internet Scene Assembler and SimVista. Files created using this integrated software are called data files and have ".in" extensions (Ishak et al. 2013, Rodriguez 2014).

DryDay.in RainOn.in

Figure 3 Sample of driving environments

Figure 3 shows a snapshot of different environments: an urban setting, and freeway settings with rain, fog and snow (not obvious from still image). The dynamics of the simulator itself can be modified by the application software SimCreator, a graphical simulation and modeling system. This software is capable of generating complex real time simulation models using a power flow style modeling method and allows for the data files created with ISA to be loaded as input connectors. Files created with SimCreator are known as model files and have ".cmp" extensions.

In addition to the data files and model files, there exist the JavaScript files with a ".js" extension. This is a lightweight, interpreted programming script with object-oriented capabilities with its core language resembling C, C++ and Java. It can be used to call up a function during the simulation to either control aspects of SimCreator (e.g. subjecting the simulator to various wind forces) or control aspects of the simulated environment (e.g. creating various intensities of ran, fog or snow).

To run experiments using the simulator, the Experimenter Interface is launched. Figure 4 shows a snapshot of this interface. The appropriate model and data files are loaded from the computers that control the simulation. The run length is the duration the simulated environment is to run. The experiment name, participant, and drive ID are chosen so that collected data can be easily

attributed to a participant and experiment. The data is stored to a specific folder and, the "distributed" option allows the simulated environment to be projected onto the projector screens. The "SimObserver" option allows the video recording to be triggered upon the simulation loading up.

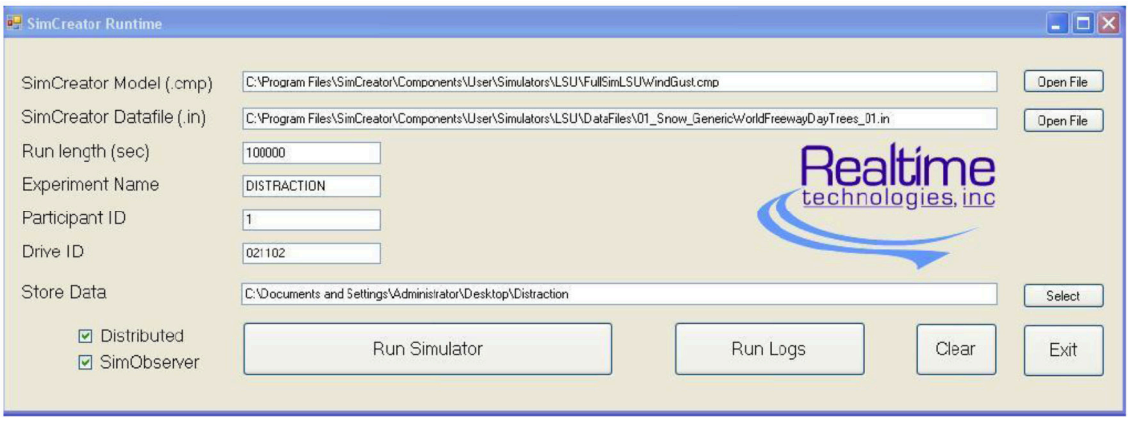

Figure 4 Experimenter interface

The simulator also has an audio software and hardware so that the participants can drive under engine sound, tire sound, and noise from the vehicle (Ishak et al. 2013, Rodriguez 2014). The driving process almost mirrors the realistic driving task of an actual vehicle. Participants have to put the car in motion, use mirrors for better visual awareness, and react to other vehicles in traffic. The simulator also reacts to changing dynamics of vehicle. In other words accelerating the simulator vehicle results in it moving forward, applying the brakes makes it lean back ward. Participants driving the simulator can sense a combined pitching motion as well as forward and rearward motion. One negative side effect of the simulator is motion sickness. Some researchers discourage the use of simulator by participant that suffers from balance disorders such as vertigo and dizziness.

3. DEFINITION AND SETTING

3.1 Aerodynamic forces of the vehicle

There are three methods used in wind engineering to study the wind effect on structures, which are wind tunnel tests, analytical approaches, and the Computational Fluid Dynamics (CFD) method. Wind tunnel tests are the most widely used way in recent decades, but it cannot implement whatever experiments the researchers expect due to its space limitation and high expense. The Computational Fluid Dynamics (CFD) method, as an alternative method to study wind effect on structures, is getting more powerful to simulate complicated flows fields, such as aerodynamic characteristics of a bridge alone and aerodynamic interaction in a vehicle-bridge-wind system. For example, Shirai and Ueda (2003) carried out aerodynamic simulations on flat box girders of a super-long-span suspension bridge by CFD method and confirmed the applicability of second-order nonlinear eddy viscosity model (k-ε model) for predicting the aerodynamic behavior in a weak irregular turbulent flow. Due to the merits of less time, financial burden, and visual production, the CFD method is adopted in this study, and the commercial CFD program Fluent is used.

The vehicle type used to simulate the aerodynamic forces is a passenger car that has similar figure with the Ford Focus installed in the simulator lab. The aerodynamic forces of the sedan are obtained under the condition of vehicle moving on the ground other than on the bridge and subjecting strong cross wind. The followed parts show basic numerical simulation information.

3.1.1 Geometry dimensions

This section presents the model geometry features that have been investigated in the current study. The shape of the vehicle determines the aerodynamic characteristics of the vehicle, which leads to some simplifications in testing aerodynamic forces of vehicles. A simplified three-dimensional geometry representing the fundamental characteristics of the flow is considered. The sedan geometry is 4.67 m long, 1.74 m wide, and 1.46 m high by neglecting some details such as railings of the bridge, pavement boards of the road surface, mirrors, and windshield wipers on the vehicle. Figure 5 shows the geometry of the sedan model.

A computational domain is defined to reflect the flow characteristics not only around the sedan model but also in the far flow field. Thus, the computational domain should be as large as the numerical simulation needed. However, the accuracy of the simulation results requires fine meshes near the model boundary so that the governing equation can be integrated from the wall boundary, which means the amount of meshes increase an order of magnitude in a 3D numerical model even when a little bit of change occurs in one dimension of the computational domain. In addition, the aerodynamic coefficients are only related to the yaw angle between the relative wind direction and the vehicle direction for a specific vehicle type. Due to the capacity of the computer, a proper computer domain was selected with 10.64 L in length, 13 L in width, and 5.5 L in height considering the vehicle running for 1 second on the road with a vehicle speed of 3 m/s, where L is the sedan length. In other words, the domain size of sedan model is 49.7 m*25.718 m*60.788 m. Figure 6 shows the geometry of the computational domain.

The domain boundaries above and below the vehicle and the bridge are set as free-slip wall boundaries, the one in front of the vehicle and the one behind the vehicle are set as symmetry boundary conditions, and the upstream boundary and downstream boundary are set as inlet and outlet boundaries, respectively, where fluids can simultaneously flow in and out of the domain. The wind velocity vector, turbulence intensity, and longitudinal scale can be specified at the inlet surface that was assigned with a uniform wind speed, turbulence kinetic energy k of 0.05, and special dissipation ratio of 2.

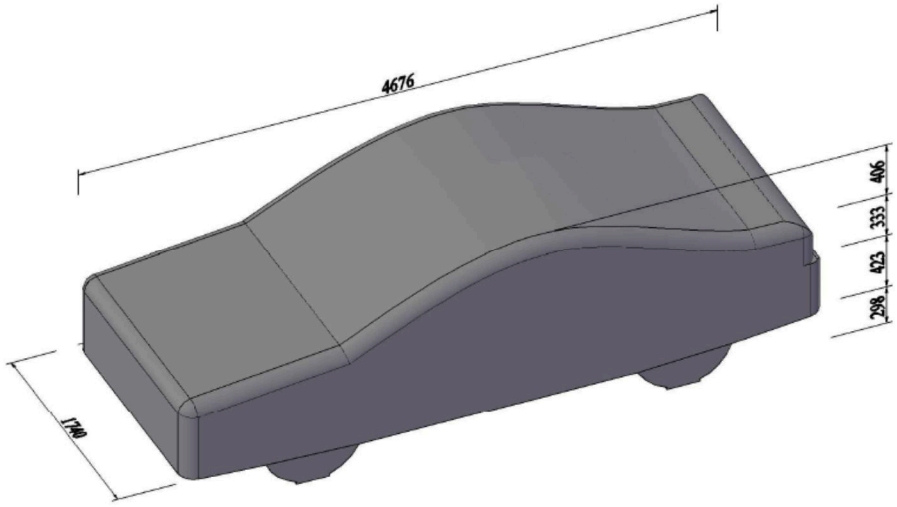

Figure 5 Geometry size of the sedan (unit:mm)

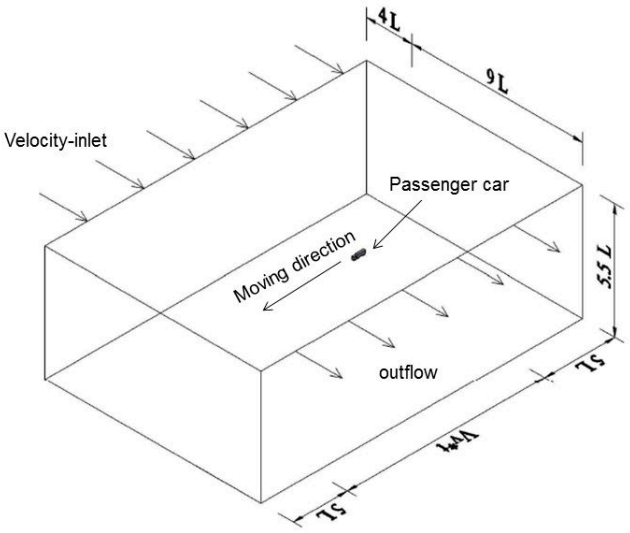

Figure 6 Computational domain

3.1.2 Numerical set-up

With the developments of computer technology, CFD has made promising progress on the application to the wind engineering (Shirai and Ueda 2003, Keerthana et al. 2011). A representative CFD program is Fluent with different type models that give the commercial software the ability to model flow, turbulence, heat transfer, and reactions for industrial applications (Fluent, 2011). There are two approaches frequently used to model the turbulence in CFD techniques: Reynolds-Averaged Navier-Stokes (RANS) models and large eddy simulation (LES). Although LES simulation can capture unsteady phenomena more accurately, it requires finer meshes and smaller time steps that cause higher computation cost than that of the RANS simulation. The RANS approach is an efficient and applicable tool to simulate the structures aerodynamics in practical wind engineering based on the time-averaged method and is a good choice to obtain the aerodynamic forces of the vehicle and the bridge. Thus, the RANS method is chosen as the simulation approach.

Reynolds (1895) proposed the Reynolds-Averaged Navier-Stokes equation based on the principle that an instantaneous quantity of fluid flow can be assembled with its time-averaged quantities and fluctuating quantities. For the incompressible airflow, after being time averaged, the Navier-Stoke equations can be described as:

$$\frac{\partial \overline{u_i}}{\partial x_i} = 0 \tag{3}$$

$$\rho\frac{\partial\overline{u_i}}{\partial t}+\rho\frac{\partial\overline{u_j}\,\overline{u_i}}{\partial x_j}=-\frac{\partial\overline{P}}{\partial x_i}+\frac{\partial}{\partial x_j}(2\mu\overline{S_{ij}}-\rho\overline{u_i'u_j'}) \tag{4}$$

Where $\overline{S_{ij}}=\frac{1}{2}(\frac{\partial\overline{u_i}}{\partial x_j}+\frac{\partial\overline{u_j}}{\partial x_i})$, $\overline{S_{ij}}$ is the modulus of the mean rate-of-strain tensor; x_i is the axis in the Cartesian coordinate system, i=1,2,3; $\overline{u_i}$ is the mean value of the velocity along the x_i direction; t is the time; ρ is the air density; $\overline{P}$ is the mean pressure of flow; μ is the air dynamic viscosity; u_i' is the fluctuating part of velocity along the x_i direction; *and* $\rho\overline{u_i'u_j'}$ is the Reynolds stress represented by the turbulence modeling, such as k-epsilon ($k-\varepsilon$) turbulence model and k-omega ($k-\omega$) turbulence model.

For bluff body aerodynamics in wind engineering, the Shear Stress Transport (SST) turbulence model has become very popular due to its good behavior for separation prediction and simulating the strong adverse pressure gradient flows (Wang 2013). The SST model is a kind of hybrid turbulence model that mixes the advantages of both *the* $k-\omega$ model and *the* $k-\varepsilon$ model. *The* $k-\omega$ model performs well for boundary layer flows, which can be integrated directly down to the wall through the viscous sub layer. On the other hand, *the* $k-\varepsilon$ model is good at dealing with free shear flow. The SST model solves turbulent kinetic energy (k) and specific dissipation rate of turbulence kinetic energy (ω) near wall, while solves k and dissipation rate of turbulent kinetic energy (ε) equation for the free stream. With introduction of a blending function, the transport equations for the SST model become:

$$\rho\frac{\partial k}{\partial t}+\rho\frac{\partial(ku_i)}{\partial x_i}=\frac{\partial}{\partial x_j}\left[\left(\mu+\frac{\mu_t}{\sigma_k}\right)\frac{\partial k}{\partial x_j}\right]+\widetilde{G_k}-\rho\beta^*\omega k \tag{5}$$

$$\rho\frac{\partial\omega}{\partial t}+\rho\frac{\partial(\omega u_j)}{\partial x_j}=\frac{\partial}{\partial x_j}\left[\left(\mu+\frac{\mu_t}{\sigma_\omega}\right)\frac{\partial\omega}{\partial x_j}\right]+\alpha\frac{\omega}{k}\widetilde{G_k}-\rho\beta\omega^2+2(1-F_1)\frac{\rho}{\omega\sigma_{\omega,2}}\frac{\partial k}{\partial x_j}\frac{\partial\omega}{\partial x_j} \tag{6}$$

$$\widetilde{G_k}=-\rho\overline{u_i'u_j'}\frac{\partial u_j}{\partial x_j} \tag{7}$$

where μ_t is the turbulent eddy viscosity; σ_k and σ_ω are the turbulent Prandtl numbers for k and ω, respectively; $\widetilde{G_k}$ is the generation of turbulence kinetic energy due to mean velocity gradients; F_1 is the blending function; *and* β^* and β are the coefficient of thermal expansion.

The present numerical simulation is conducted with the SST model, in which the turbulent eddy viscosity is computed as follows (Fluent 2011):

$$\mu_t = \frac{\rho k}{\omega} \frac{1}{\max\left[\frac{1}{\alpha^*}, \frac{SF_2}{a_1 \omega}\right]} \tag{8}$$

and σ_k and σ_ω are calculated by

$$\sigma_k = \frac{1}{F_1/\sigma_{k,1} + (1-F_1)/\sigma_{k,2}} \tag{9}$$

$$\sigma_\omega = \frac{1}{F_1/\sigma_{\omega,1} + (1-F_1)/\sigma_{\omega,2}} \tag{10}$$

where S is the strain rate magnitude; the coefficient α^* damps the turbulent viscosity causing a low-Reynolds number correction. Model constants used in Fluent are listed below. $\sigma_{k,1} = 1.176$;$\sigma_{\omega,1} = 2.0$ $\sigma_{k,2}$=1.0;$\sigma_{\omega,2} = 1.168$ and a_1=0.31.

Fluent, a popular CFD software, was adopted to solve the equations in single precision. The finite volume method was used to discretize the governing equations in this study. Momentum, Turbulent Kinetic Energy and Specific Dissipation Rate were discretized using the Quick. The pressure was discretized in standard scheme. Gradient terms were handled by the use of the Least Squares Cell Based approach. The PISO algorithm was employed for velocity and pressure coupling. To carry out the dynamic mesh technology in the numerical simulation, a user defined file (UDF) was compiled with the Fluent setup, which means the Transient Formulation can only be performed using the first-order implicit method. At each time step, the results were accepted as convergent after 20 iterations. Figure 7 shows the solution method setting in Fluent and Figure 8 is the snapshot of the UDF.

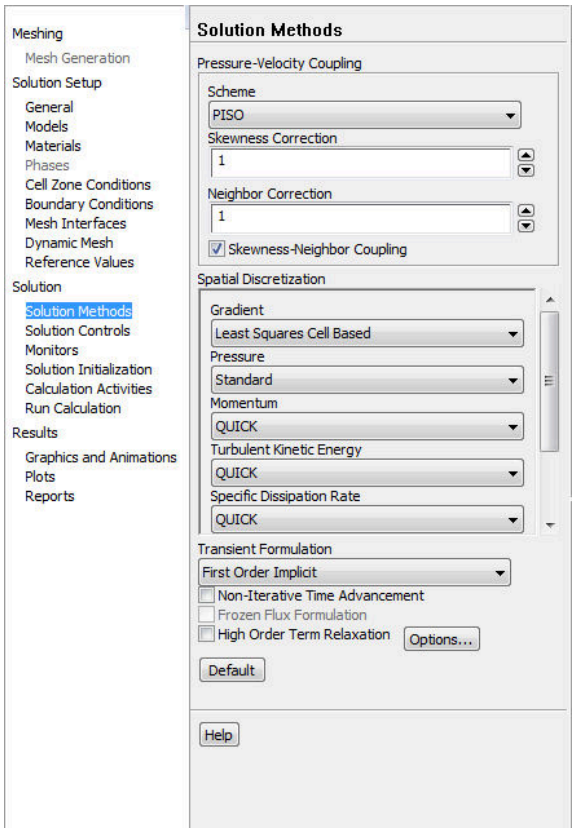

Figure 7 Snapshot of Fluent solution panel

```
DEFINE_CG_MOTION(sedan,dt,vel,omega,time,dtime)
{

        Domain * domain ;
        Thread*tf=DT_THREAD(dt);
        face_t f;
        t=time;
        dt1=dtime;
        t=t+dt1;

      if(t<2.0)
      {
         vel[0]=v_prev;
       }
      else
       {
         vel[0]=0.0;
        }

domain = THREAD_DOMAIN (DT_THREAD ((Dynamic_Thread *)dt));
tf = Lookup_Thread(domain,32);
 body_centroid[0]=DT_CG(dt)[0];
 body_centroid[1]=DT_CG(dt)[1];
 body_centroid[2]=DT_CG(dt)[2];

 Compute_Force_And_Moment(domain,tf,body_centroid,force,moment,TRUE);

 C_force[0]=force[0]/(0.5*F_density*U_flow*U_flow*area);
 C_force[1]=force[1]/(0.5*F_density*U_flow*U_flow*area);
 C_force[2]=force[2]/(0.5*F_density*U_flow*U_flow*area);
```

Figure 8 Snapshot of the UDF

3.1.3 Definition of aerodynamic forces of vehicle

Quasi-static wind forces on vehicles are widely used in predicting wind forces of vehicles both in static situation and in running condition since a transient type of force equations for vehicles are not available. The aerodynamic forces and moments are defined as follows:

$$F_d = 0.5\rho C_d V^2 A \quad \text{Drag force,} \quad (11a)$$

$$F_l = 0.5\rho C_l V^2 A \quad \text{Lift force,} \quad (11b)$$

$$F_s = 0.5\rho C_s V^2 A \quad \text{Side force,} \quad (11c)$$

$$M_r = 0.5\rho C_r V^2 AL \quad \text{Rolling moment,} \quad (11d)$$

$$M_y = 0.5\rho C_y V^2 AL \quad \text{Yawing moment,} \quad (11e)$$

$$M_p = 0.5\rho C_p V^2 AL \quad \text{Pitching moment,} \quad (11f)$$

Where ρ is the density of air, A is the frontal area of the vehicle, V is the resultant wind speed, and Cd, Cl, Cs, Cr, Cy, and Cp are aerodynamic coefficients. The positive direction of these wind forces is shown in Figure 9. Figure 10 illustrates the resultant velocity of the wind direction due to the vehicle motion, where Vv shows the vehicle moving direction, and U shows the wind direction.

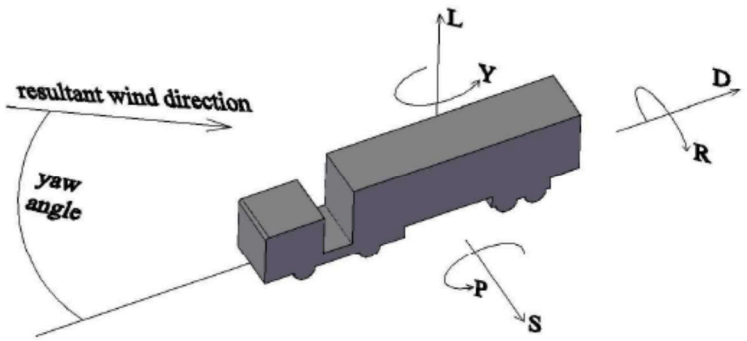

Figure 9 Sign convention for aerodynamic forces of the vehicle

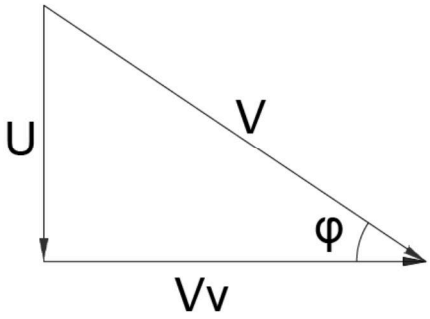

Figure 10 Velocities and direction

There is adequate experimental data to estimate the wind force coefficients of the vehicle concerning the open ground scenario (Baker 1991a, Quinn et al. 2007). Most of the coefficients are described as a function of the yaw angle between the resultant wind direction and the vehicle

driving direction, such as the research conducted by Baker (1987). The coefficients of vehicle aerodynamic characteristics are shown below.

Side force coefficient $$C_s(\varphi) = a_1(\varphi)^{0.382} \quad (12a)$$

Lift force coefficient $$C_l(\varphi) = a_2(1 + sin3\varphi) \quad (12b)$$

Drag force coefficient $$C_d(\varphi) = -a_3(1 + 2sin3\varphi) \quad (12c)$$

Yawing moment coefficient $$C_y(\varphi) = -a_4(\varphi)^{1.77} \quad (12d)$$

Pitching moment coefficient $$C_p(\varphi) = a_5(\varphi)^{1.32} \quad (12e)$$

Rolling moment coefficient $$C_r(\varphi) = a_6(\varphi)^{0.294} \quad (12f)$$

3.2 Simulator test

3.2.1 Modification of dynamics of the LSU driving simulator

In the simulator test, an average size sedan was selected to be exposed in sustained wind. The basic geometry dimension of the sedan was introduced in section 3.1.1, and the weight of the sedan is estimated as 1318 kg. SimVhicleLT™ was used to create different vehicle profiles using the GUI (Graphic User Interface) editing system. This system uses ".NET" technology and an excel spreadsheet to create the models needed as shown in Figure 11. According to the vehicle's number of axles and characteristics (mass, suspension, aerodynamics, brake data, etc.), a data file was generated and loaded into the simulator for the vehicle type to represent its behavior (Rodriguez 2014).

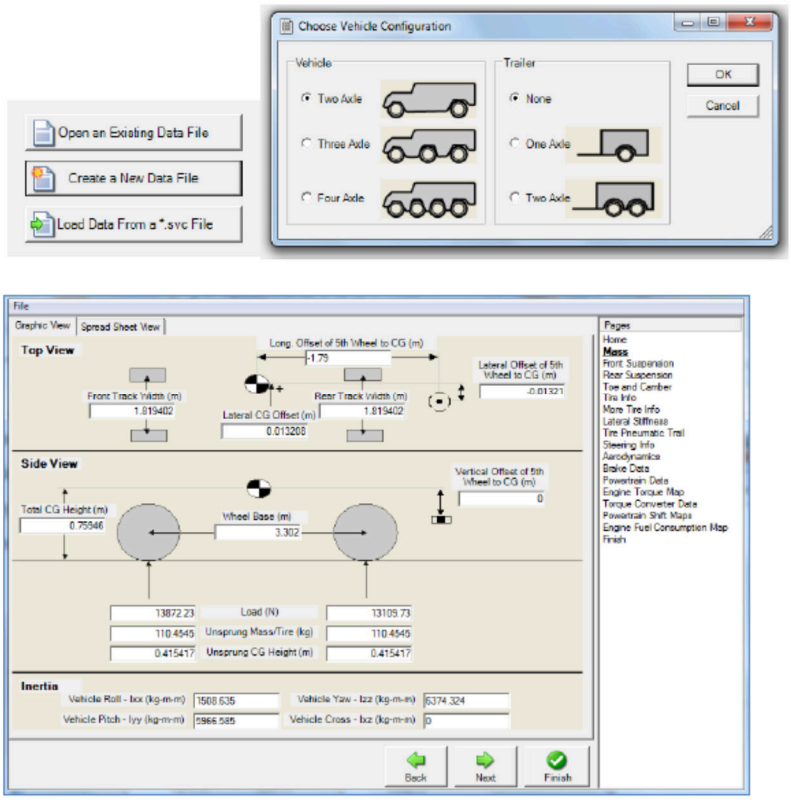

Figure 11 SimVehicleLT™, GUI editing system

3.2.2 Design of sustained winds and rainfall

The sustained wind speeds used for the study were taken from the Saffir-Simpson Hurricane wind scale as shown in Table 1. The wind speeds for the 1 min sustained hurricane wind scale were observed and estimated at the standard meteorological height of 10 m (33 ft.) in an unobstructed exposure (NOAA 2008, Rodriguez 2014). However, they were converted to wind speed on a vehicle about 1 m above the ground with the following equation:

$$U_1 = U_2 ln(^{z_1}/_{z_0})/ln(^{z_2}/_{z_0}) \quad (13)$$

Although the wind profile in the lowest layer is uncertain, the log law wind profile in the equation is commonly used to estimate wind speed U_1 at height z_1 from known wind speed U_2 at height z_2 using a roughness length z_0 (Stull 1988, 1995). In this study, the sedan was supposed to be running on an open ground freeway where farm fields were located, thus, the roughness length becomes 0.01 m. Under that condition, the wind speed at 1 m height is about 0.67 of the wind speed at 10 m height.

Wind speed of the hurricane Category II of the SSHWS was selected to mimic the hurricane strong wind, which means the wind speed were 43-49 m/s. Conversions were made

between this 10 m height wind speed and 1m height wind speed, and the magnitude of 30 m/s was determined for the 1m height wind velocity. The direction of the wind speed was always perpendicular with the centerline of the straight freeway.

Considering the fluctuation of mean wind speeds, two types of wind conditions were taken into account on a certain degree of simplifications as shown in Figure 12. For the 30 m/s wind speed at 1 m height, one scenario was the vehicle suddenly subjecting a constant wind for 40 s; the other one was subjecting a changed wind for 60 s total. In the second wind type, there were four 15 s changed wind with different directions. In each changed wind period, the time of 15 s was divided into 5 parts evenly, and the wind speed was 10 m/s in the first and last part, in the second and the forth part it was 20 m/s, and it was 30 m/s in the middle part. To control the duration of the strong wind, time sensors were used in the scenario creation in *SimVista* software. Time sensors generate continuous events at programmed points in time by modifying the time sensor properties of the object property dialog box. The notion of a start time and a stop time making an event can be created at any specific time. In fact, wind effects were continuous events and expected to be enabled between the start time and the stop time. For the 40 s wind type 1, there was only one time sensor needed since wind speed is kept constant while there were five time sensors used in the 15 s wind type 2 scenario due to the alternation of wind speed.

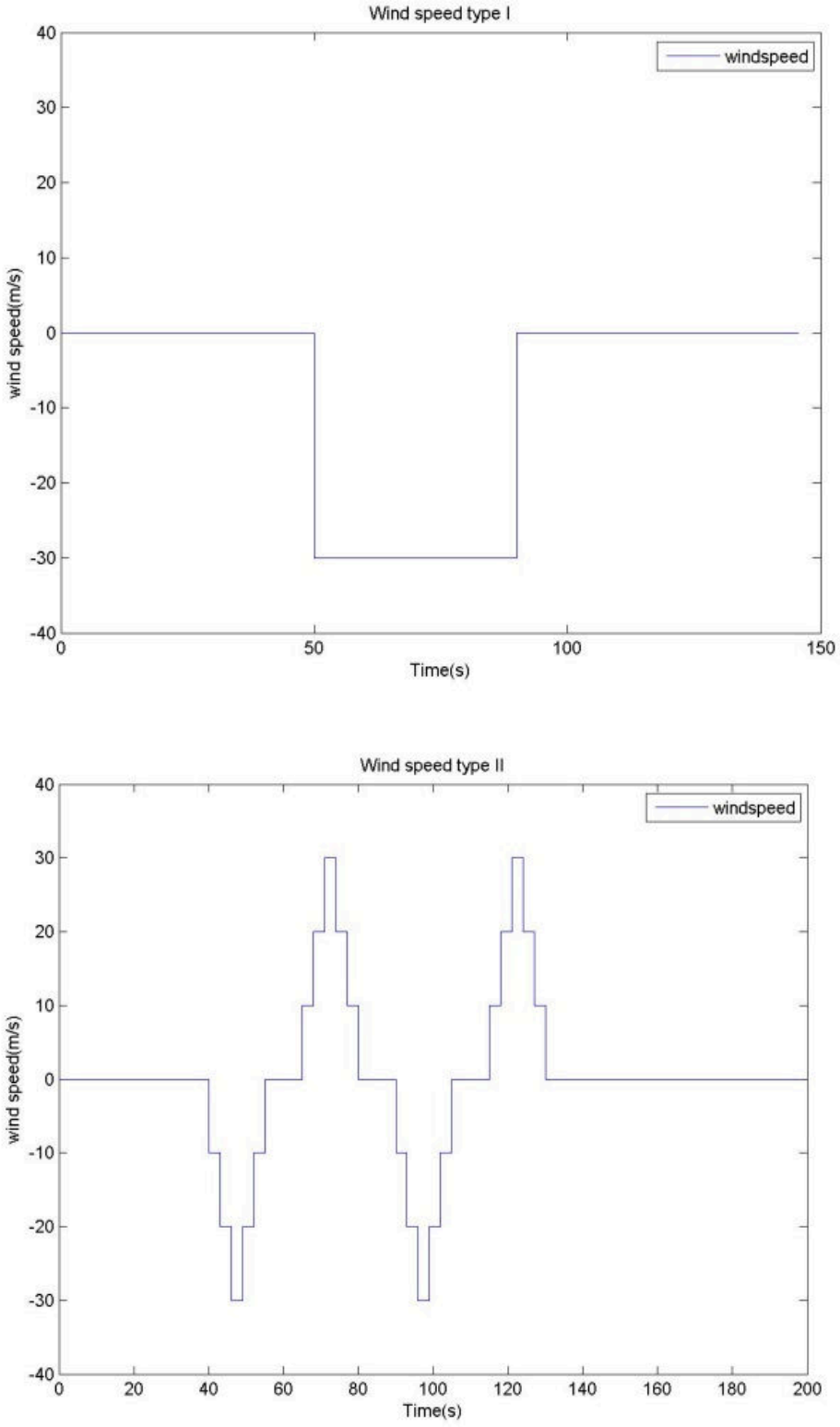

Figure 12 Wind types used in the simulator tests

To investigate the effect of rainy weather on the vehicle performance, a rainy weather parameter was setup in the simulator environment file. The scenario projected on the front screen can illustrate the raindrop with a constant rainfall volume so that the driver can sense a rainy environment.

On the vehicle characteristics, the influence of the wet road surface on the vehicle was exercised by setting a friction factor between the vehicle tire and the road surface. In accordance with the speed limit of the highway, 65 mph, and the road surface condition, the friction value of 0.5 was chosen for wet road surface and 1.0 was selected for dry road surface under the supposition of worn tire condition (Robert Bosch GmbH 1996).

3.2.3 Modification of JavaScript File and data file in SimCreator

As noted in the background section, the ".cmp" model files, ".in" data files, and ".js" JavaScript files work together during any simulation event. The ".cmp" files are in charge of the vehicle driving simulator in that they manage all the processes related to the vehicle performance during the simulation. The ".in" files manage the scenario and handle the environment of the vehicle. ".js" files are used to alter vehicle and scenario characteristics through JavaScript program.

For the purpose of this study, a ".js" file was developed to manage the magnitude of the wind force applied to the vehicle. In this file, magnitude of the wind force was calculated by the wind force equation generated based on the simulation results, which are related to the magnitude of wind speed and vehicle velocity. Figure 13 shows a part of ".js" file of an example of scenario that a constant 30 m/s wind blows on the vehicle. The ".js" file was assigned to a time sensor in order to control the wind effect in the time sensor duration. Thus, the valid time of the wind force is the active time of the time sensor. For example, a time sensor was set to start at 30 s and stop at 50 s, and then the vehicle was affected during 30 s-50 s by the wind type designated by a ".js" file. The syntax of Scenario.Subject.getVelocity() means to get the vehicle velocity 60 times in a minute. Based on the vehicle velocity and wind speed, we can get console output of the yaw angle of the resultant wind velocity, and the wind forces. Wind forces were converted into two-dimensional forces and applied to the vehicle so the effect on the driving behavior of test subjects may be observed. The vector SimCreator.WindForce.SignIn[1] represents lateral forces while SimCreator.WindForce.SignIn[0] represents longitudinal forces.

As mentioned in section 3.2.2, the two type winds were sustained for 30 s and 15 s, respectively, and one time sensor was set for 30 s wind scenario and five time sensors were used for the 15 s wind environment. In the 15 s type wind, only three ".js" files were needed to attach to the five time sensors since both 10m/s wind can share a ".js" file. Therefore, four ".js" files were created to assign to corresponding time sensors.

```
<meta charset="UTF-8">
<title>Insert title here</title>
<script type="text/javascript">
        var Da = 1.225, Vw = 30, A = 2.57;
        var a1 = 1.6, a2 = 0, a3 = 0.25;
        var q = 0.5*Da*A;
        var Vv = Scenario.subject.getVelocity();
        var VSquared = Vw*Vw+Vv*Vv;
        var angle = Math.atan(Vw / Vv);
        var Cs = a1*Math.pow(angle, 0.382);
        var Cl = a2*(1+Math.sin(angle));
        var Cd = -a3*(1+2*Math.sin(3*angle));
        var Fs = q*VSquared*Cs;
        var Fl = q*VSquared*Cl;
        var Fd = q*VSquared*Cd;
        function calculate(){
                console.log("q = " + q);
                console.log("VSquared = " + VSquared);
                console.log("angle = " + angle);
                console.log("Cs = " + Cs);
                console.log("C1 = " + Cl);
                console.log("Cd = " + Cd);
                console.log("Fs = " + Fs);
                console.log("F1 = " + Fl);
                console.log("Fd = " + Fd);
        }
/*
        simCreator.WindForce.SigIn[0] = Fs;
        simCreator.WindForce.SigIn[1] = Fl;
        simCreator.WindForce.SigIn[2] = Fd
*/
</script>
</head>
<body onload="calculate()">
```

Figure 13 A part of ".js" file for a time sensor

As mentioned above, the ".in" file was utilized to control the scenario and driving environment. Thus, the successful demonstration of the rainfall in the driving scenario was only needed to change the data file. Figure 14 shows a part of final data file for rainy environment. In all components including center channel, right channel, left channel, rear channel and side mirrors, visual setting of rain line number, rain width and rain lighting were added through syntaxes of *rain[0][0], rain[0][1], rain[0][2],* respectively. On the other hand, the slid friction between the vehicle tires and the road surface is a key parameter in vehicle slip away events. In the data file, the friction was also changed to 0.5 to mimic the reduction of adhesive force of the tire on a wet surface.

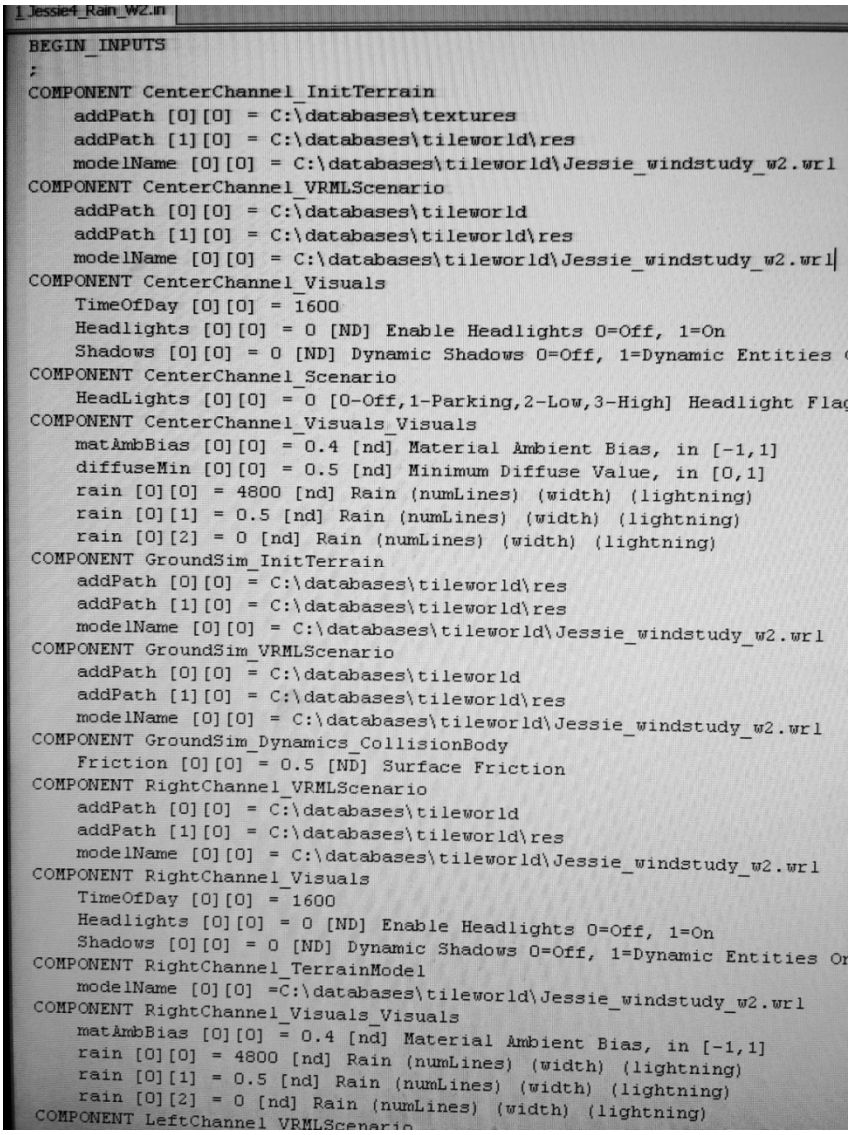

```
1 Jessie4_Rain_W2.in
BEGIN_INPUTS
;
COMPONENT CenterChannel_InitTerrain
    addPath [0][0] = C:\databases\textures
    addPath [1][0] = C:\databases\tileworld\res
    modelName [0][0] = C:\databases\tileworld\Jessie_windstudy_w2.wrl
COMPONENT CenterChannel_VRMLScenario
    addPath [0][0] = C:\databases\tileworld
    addPath [1][0] = C:\databases\tileworld\res
    modelName [0][0] = C:\databases\tileworld\Jessie_windstudy_w2.wrl
COMPONENT CenterChannel_Visuals
    TimeOfDay [0][0] = 1600
    Headlights [0][0] = 0 [ND] Enable Headlights 0=Off, 1=On
    Shadows [0][0] = 0 [ND] Dynamic Shadows 0=Off, 1=Dynamic Entities
COMPONENT CenterChannel_Scenario
    HeadLights [0][0] = 0 [0-Off,1-Parking,2-Low,3-High] Headlight Flag
COMPONENT CenterChannel_Visuals_Visuals
    matAmbBias [0][0] = 0.4 [nd] Material Ambient Bias, in [-1,1]
    diffuseMin [0][0] = 0.5 [nd] Minimum Diffuse Value, in [0,1]
    rain [0][0] = 4800 [nd] Rain (numLines) (width) (lightning)
    rain [0][1] = 0.5 [nd] Rain (numLines) (width) (lightning)
    rain [0][2] = 0 [nd] Rain (numLines) (width) (lightning)
COMPONENT GroundSim_InitTerrain
    addPath [0][0] = C:\databases\tileworld\res
    addPath [1][0] = C:\databases\tileworld\res
    modelName [0][0] = C:\databases\tileworld\Jessie_windstudy_w2.wrl
COMPONENT GroundSim_VRMLScenario
    addPath [0][0] = C:\databases\tileworld
    addPath [1][0] = C:\databases\tileworld\res
    modelName [0][0] = C:\databases\tileworld\Jessie_windstudy_w2.wrl
COMPONENT GroundSim_Dynamics_CollisionBody
    Friction [0][0] = 0.5 [ND] Surface Friction
COMPONENT RightChannel_VRMLScenario
    addPath [0][0] = C:\databases\tileworld
    addPath [1][0] = C:\databases\tileworld\res
    modelName [0][0] = C:\databases\tileworld\Jessie_windstudy_w2.wrl
COMPONENT RightChannel_Visuals
    TimeOfDay [0][0] = 1600
    Headlights [0][0] = 0 [ND] Enable Headlights 0=Off, 1=On
    Shadows [0][0] = 0 [ND] Dynamic Shadows 0=Off, 1=Dynamic Entities Or
COMPONENT RightChannel_TerrainModel
    modelName [0][0] =C:\databases\tileworld\Jessie_windstudy_w2.wrl
COMPONENT RightChannel_Visuals_Visuals
    matAmbBias [0][0] = 0.4 [nd] Material Ambient Bias, in [-1,1]
    rain [0][0] = 4800 [nd] Rain (numLines) (width) (lightning)
    rain [0][1] = 0.5 [nd] Rain (numLines) (width) (lightning)
    rain [0][2] = 0 [nd] Rain (numLines) (width) (lightning)
COMPONENT LeftChannel_VRMLScenario
```

Figure 14 A part of the data file

3.2.4 Experiment procedure

To investigate the vehicle's performance under inclement weather including hurricane wind and rainfall, a driver's reaction should be studied. Each driver behaves differently when encountering similar environments, even an exact same scenario. This study was aimed on the performance of the vehicle and the behavior of each driver when subjected to the same scenario in different days. There were only two persons recruited for this study as there were only two wind conditions generated. Each driver drove one time in the wind scenario and one time the wind-rain scenario ten times in a month. Driver's behaviors on the same environmental condition were focused on and analyzed in the following section.

The test consisted of four stages and lasted approximately fifteen minutes every day. The first part was the introduction in which participants were briefed on the experiment and asked to sign the consent sheet. Participants were then asked to randomly arrange a selection of cards to determine the order of the two weather conditions they were tested on. The second stage was the training stage. Participants were allowed to operate the driving simulator until a time that they felt adapted to the controls and displays of the vehicle. In the next part, the test stage, drivers were asked to drive in the right lane throughout the tests. In each wind condition, the vehicle was exposed to several 90^0-winds, and the wind force was applied on the vehicle based on the vehicle velocity. In both non-rainy and rainy weather conditions; a test phase normally lasted three minutes. After the phase of the first weather condition, drivers were asked to stop at the stop sign, and then the test repeated with the phase of the second weather condition. The final part consisted of answering a short questionnaire. Questions included personal information such as age and driving experience. Other information obtained included qualitative assessment of the participant's experience during the experiment.

With a sampling rate of 60 Hz, the output file generated by SimObserver for each experimental condition contained the corresponding video clip and data on time, heading error, engine's RPM, and trajectory offset that were used to analyze the driving behavior of participant for the experiment. The experimenter's interface, shown in Figure 4, was the interface used to run each experiment for SimObserver to collect the corresponding data. The participant ID and Driver ID were unique in determining which experimental condition was being tested. The output ".dat" file was by default named with the drive ID unique number, so that it was easy to distinguish among the files. Figure 15 shows a snapshot of the output data, comprising the synchronized video and sequential data file, for one experimental condition during the test.

Figure 15 Sample output data file from SimObserver

3.2.5 Selected variables

Data was collected on several performance variables: the lane offset (a), driver steering angle (δ), and vehicle velocity (V_v). The lane offset is defined as the lateral displacement between the longitudinal central lines of the vehicle in the initial status and in the motion status shown in Figure 16. This variable gives an indication of the level of lateral control that a participant has over the vehicle. A larger absolute value of lane offset indicates less lateral control of the simulator and vice versa. The driver's steering angle is recorded as the manipulation of the driver applied on the steering wheel in the form of an angle. This variable gives an indication of the driver's behavior of adjusting a vehicle heading in a straight lane.

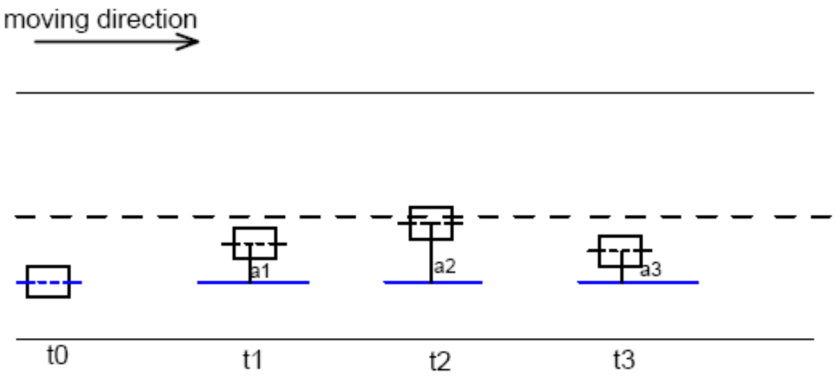

Figure 16 Definition of the lane offset of the vehicle

Table 4 provides a truncated snapshot of the data collected for each driving participant. For each wind type, the average estimates of the lane offset, steering angle, and vehicle velocity corresponding to each time point were calculated for all test times using MATLAB. The average estimates on the variables were used to comparatively analyze how the participants react and responded to the wind force.

The resulting mean data for each time point can be denoted as $\overline{x_l}$ and estimated using the equation:

$$\overline{x_l} = \frac{\sum_{i=1}^{n} x_{il}}{n} \tag{14}$$

Where $l = performace\ variable = \begin{cases} 1, lane\ offset(\alpha) \\ 2, steering\ angle\ (\delta) \\ 3, vehicle\ velocity\ (V_v) \end{cases}$

$$n = times\ of\ tests$$

Table 4 Truncated data sheet collected by SimObserver

Simulation time	Lane Offset	Steering angle	Longitudinal Velocity
83.3905	-0.04857	1.841493	29.98281
83.4072	-0.0505	1.905259	29.983
83.4239	-0.05239	1.951385	29.98318
83.4406	-0.05424	1.97789	29.98336
83.4572	-0.05605	1.989425	29.98354
83.4739	-0.05781	1.988349	29.98372
83.4906	-0.05952	1.976696	29.98394
83.5073	-0.06119	1.962053	29.98419
83.524	-0.06281	1.944494	29.98448
83.5407	-0.06439	1.915537	29.98477
83.5573	-0.06591	1.874101	29.98506

At any time, the lateral displacement (Δ) is defined as the difference in the lane offset caused by a change in the lateral wind. The a_1 represented the initial position when the wind applied to the vehicle; a_2 was the final position before the driver reacted for lane offset correction.

$$\Delta(t) = a_2(t_2) - a_1(t_1) \tag{15}$$

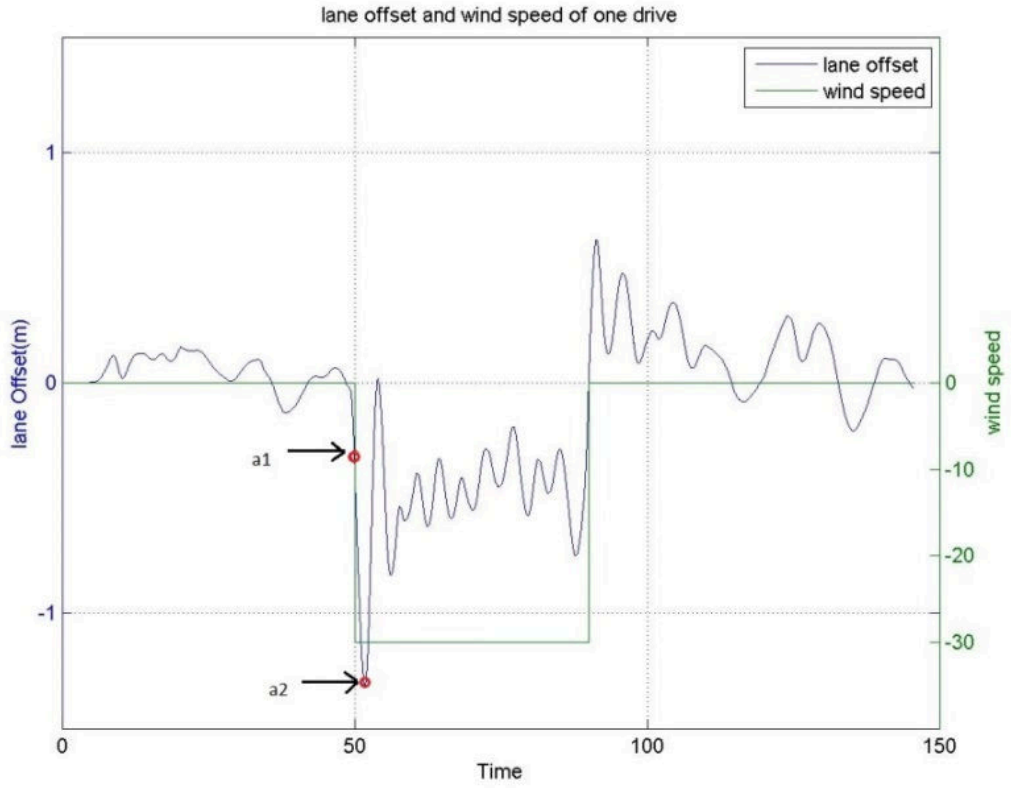

Figure 17 Lane offset and wind speed for one drive

Figure 17 shows the lane offset and applied wind for one of the participant's driving in the second wind condition during the 150 s. During the first 50 s no wind forces are applied and the lane offset is lower than 0.5 m. The first hit of wind on the vehicle happened at 50 s of simulation when the vehicle has a lane offset of a_1 as the vehicle is displaced, and then a proper operation makes a lane offset compensation that occurred at lane offset of a_2. The difference between the two lane offset was defined by the lateral displacement of vehicle due to the wind as discussed earlier.

The vehicle's sideslip time due to the strong cross wind is detected by comparing the end time of first lateral displacement due to the strong wind. In Figure 17, the difference of the times when

vehicle at a_1 position and a_2 position are considered as the vehicle's sideslip time because the absolute lane offset became smaller at the end of side slipping. In other words, the compensation of trajectory off symbolizes the completion of the vehicle side slipping and the vehicle sideslip time caused by the strong wind can be calculated by subtracting the wind starting point time from the trajectory off compensating point time. Figure 18 shows the lane offset of the vehicle from 50 s to 53 s. As in conjunction with Figure 17, the road off correction by the driver operation occurred a little later than the wind-applied time.

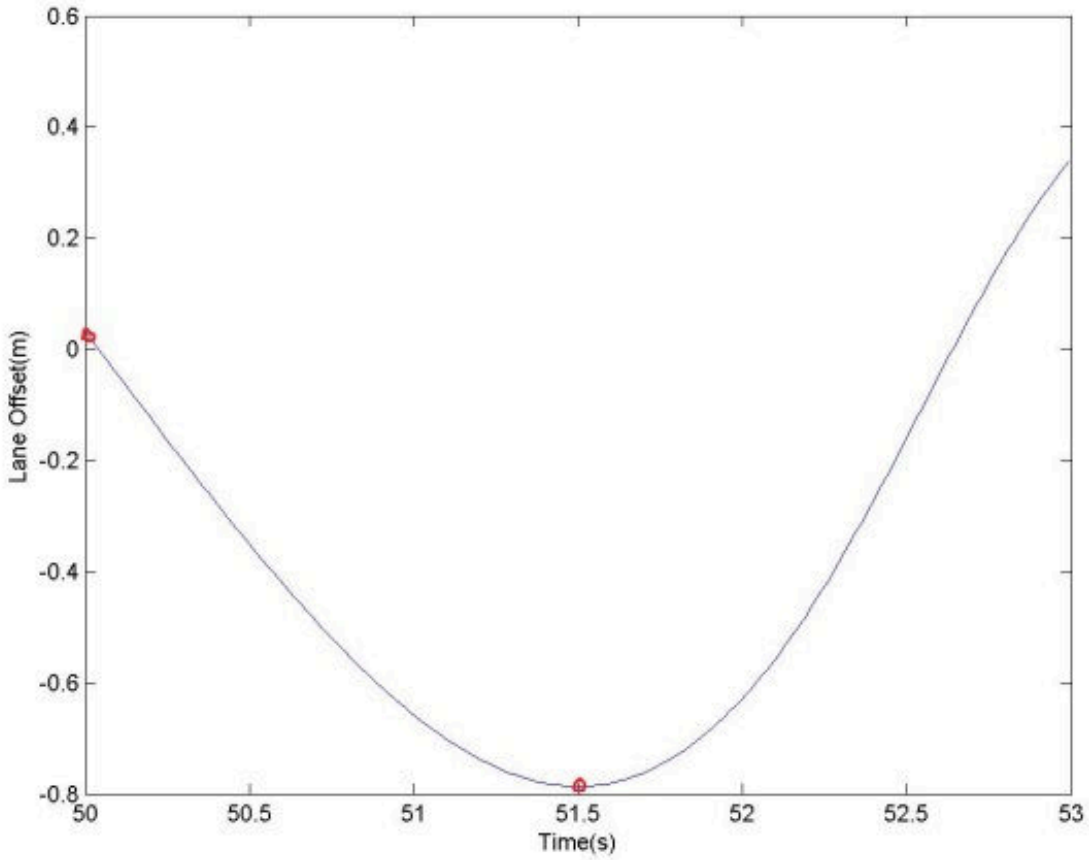

Figure 18 Lane offset between 50 s-53 s

The driver's proper operation stops the vehicle sideslip from increasing lateral displacement, thus the driver's behavior happens during the vehicle side slipping. From the vehicle trajectory, it is hard to distinguish the driver's reaction time because the vehicle keeps slipping for a little while after the heading error correction. However, video record can be used to help recognize the driver's reaction. Cameras installed in the car cab record the driver's behavior during every driving procedure including how the driver steers the steering wheel and pushes

brake and gas pedals. Figure 15 is an example of the still image from the video and the synchronized vehicle data including the simulation time, the vehicle position, the vehicle velocity, the steering angle, and the heading error. Reviews on video record indicated that the driver turned the steering wheel while the vehicle course deviates, and there was an obvious turn of the steering wheel under the driver behavior. Figure 19 shows the relative steering angles of the steering wheel under the driver's manipulation in different points of time and reveals the driver's behavior when encountering strong wind. There are two red lines in assistance to observe the variance of the steering angle; one is to stand for the steering wheel and another represents the dashboard of the vehicle. Figure 19 (a) is captured from the video record at 50 s when the strong wind forces are applied on the vehicle. At that time, the driver was considered keeping regular driving without sudden operation due to the two red lines are almost parallel. At time of 50.815 s, shown in Figure 19 (b), the relative angle between the two red lines were changed, which means the driver tried to turn the steering wheel to correct the heading error. During the strong wind period, the driver has to turn a certain steer angle to keep the vehicle from course deviation, as shown in Figure 19 (c).

(a) T=50.000 s

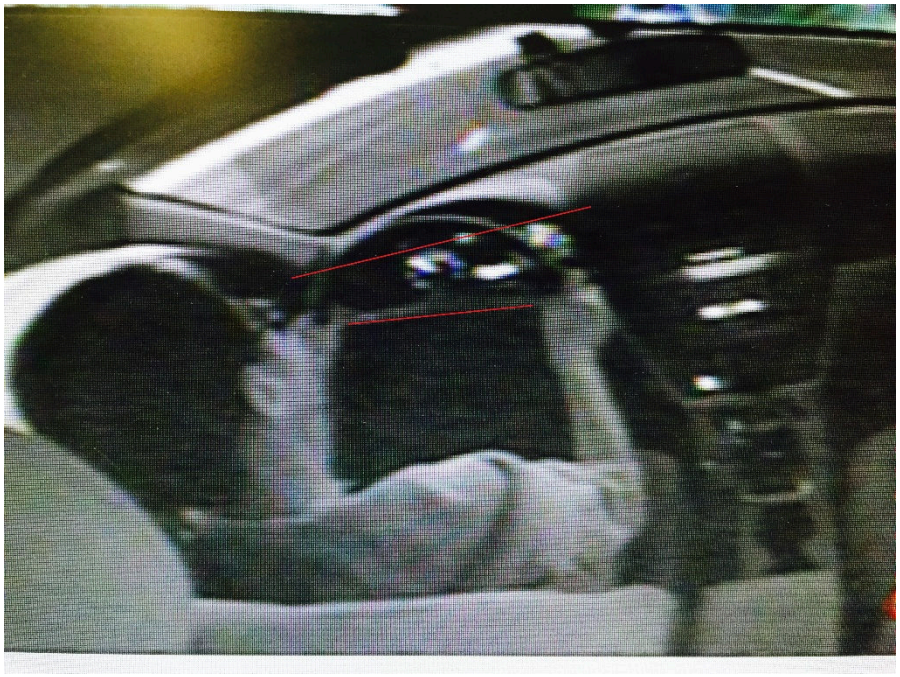

(b) T=50.815 s

(c) T=52.015 s

Figure 19 Steer angle in different moments

4. RESULTS AND DISCUSSION

4.1 Results of the numerical simulation

To obtain a similar expression of the aerodynamic coefficients of the moving car with those of the static truck (Baker 1987), different yaw angles were studied, such as 30^0, 45^0, 60^0, and 75^0 corresponding to the wind speed of 1.732 m/s, 3 m/s, 5.196 m/s, and 11.2 m/s, respectively. The yaw angle of 90^0 means that the vehicle stayed static in the wind flows. The mesh numbers of each yaw angle case become 4.63 million, 4.74 million, 4.86 million, and 5.02 million, respectively. Finally, the huge numerical computations were conducted on the 8 nodes 128 cores of the MIKE in the High Performance Computing center at Louisiana State University.

4.1.1 Time history of aerodynamic force coefficients

Figure 20 shows the time history of the six aerodynamic coefficients of a moving vehicle at a yaw angle of 30^0. The simulation time was 2 seconds total containing a 0.5 s static situation, 1 s for vehicle moving condition, and 0.5 s of the second static situation. From the time history of the aerodynamic coefficients, it can be seen that the value of each coefficient keeps fluctuating around a mean value as the time increases, and a duration of 1 s was sufficient to obtain the mean value of each coefficient. It can be seen that there are obvious differences between the coefficients of the static vehicle and the moving vehicle. Compared with the coefficients of the static vehicle under the same wind condition, the lift force, side force, and pitching moment coefficients decrease when the vehicle runs, while the drag force and rolling moment coefficients increase. In both static situations before and after the motion, five aerodynamic coefficients trend to have similar values, respectively, except the rolling moment coefficient, which indirectly indicates that the simulation results are acceptable.

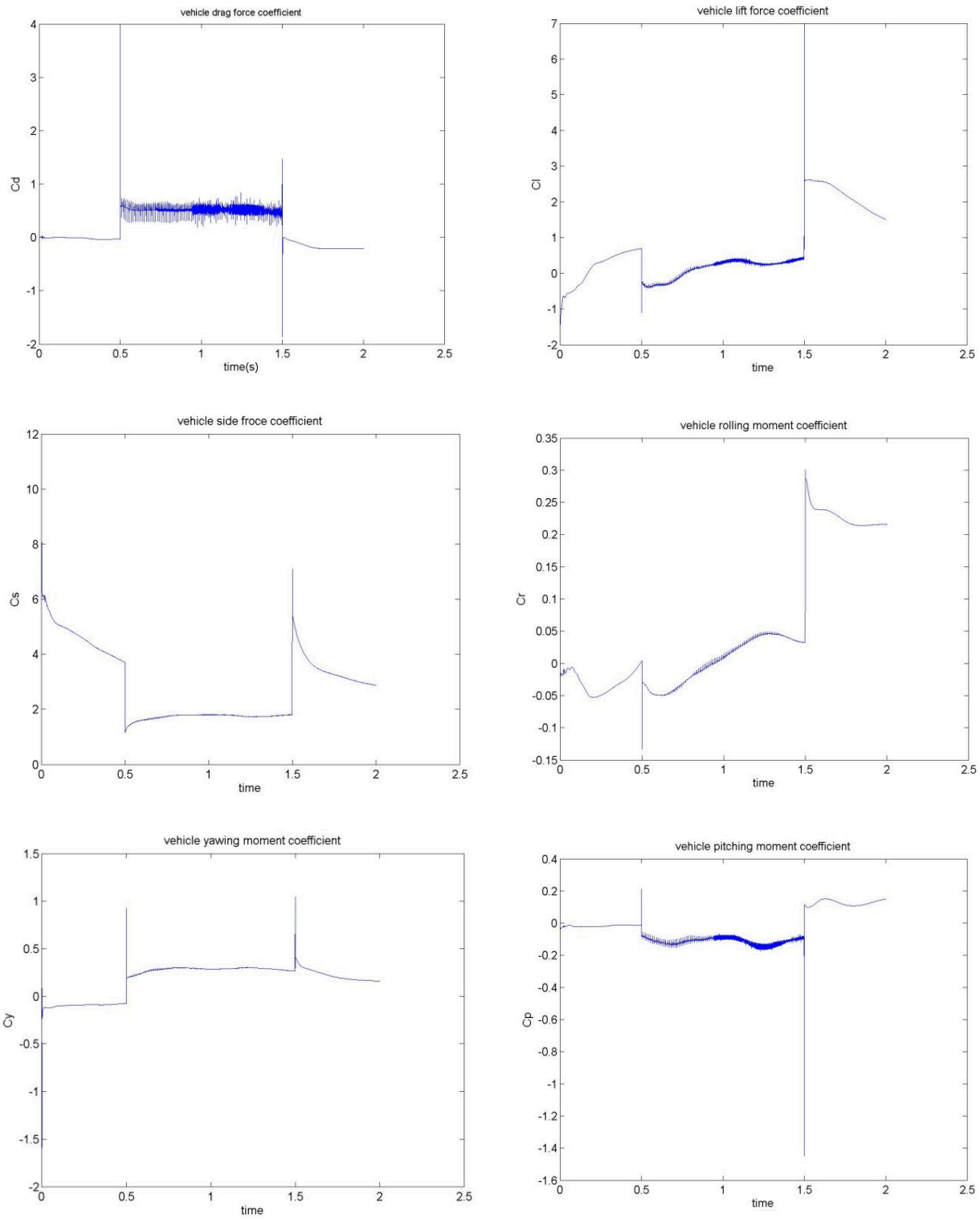

Figure 20 Aerodynamic coefficients of vehicle

4.1.2 Mean force coefficients of the sedan

Aerodynamic coefficients of the sedan running on the open road under windy environment were obtained through the numerical simulation method. The mean values of the coefficients under four yaw angles are listed in Table 5. The variation of the aerodynamic coefficients of the sedan ranging from 30°-90° yaw angle can be seen in Table 5. The side force coefficient Cs increases with the yaw angle and reaches the maximum value at 90° while the drag force coefficient Cd decreases with the yaw angle and reaches the minimum value at 90°. The lift force coefficient increases first and then decreases, reaching the maximum value around the 60^0 yaw angle. The mean value of the side force coefficient reduced to 1.799 from 2.796 after starting to move by a percentage of around 36%, and the mean value of the lift force coefficient was 0.758 under the static situation and decreased to 0.404 by a percentage of 47%. There is no general law for the moment coefficients against the yaw angles due to the complicated impact factors such as different forces and points of action.

Table 5 The mean aerodynamic coefficients of the sedan in different yaw angels

Yaw angle	Cd	Cl	Cs	Cr	Cy	Cp
30^0	0.4679	0.4047	1.7998	0.0330	0.2680	-0.0931
45^0	0.3924	0.6615	2.4251	0.0547	0.2802	-0.0649
60^0	0.1811	0.9549	2.6953	0.0597	0.1567	-0.0991
75^0	-0.0280	0.7311	2.7008	0.0003	0.0594	-0.0391
90^0	-0.0941	0.4827	2.7966	0.0652	-0.0221	0.0268

Based on the wind tunnel experiment results, Baker (1987) proposed the formulae of the aerodynamic force and moment coefficients of standard vehicles over a yaw angle range between 0^0 and 180^0; these equations were in forms of the sine functions and exponential functions as shown in Equation 12. In addition, Han et al. (2014) proposed the wind force coefficients formulae of the vehicle on the bridge by fitting the experimental data obtained from the previous wind tunnel tests (Han et al., 2013), in which only sine functions were used. Assuming that the same form of the variation of the forces and moment coefficients with the yaw angle is valid for this sedan type, aerodynamic coefficients of a running sedan under cross wind are proposed through fitting the simulation results with the sine function of yaw angle as:

For $0 \leq \varphi \leq \pi/2$

$$Cd = 0.1862 - 0.0543 * cos(0.0559 * \varphi) + 0.2774 * sin(0.0559 * \varphi) \quad \text{Drag} \quad (16a)$$

$$Cl = 0.6888 + 0.2537 * cos(0.0995 * \varphi) - 0.0387 * sin(0.0995 * \varphi) \quad \text{Lift} \quad (16b)$$

$$Cs = 2.813 * sin(0.0178 * \varphi + 0.1808) \quad \text{Side} \quad (16c)$$
$$Cr = 0.4376 - 0.0234 * \cos(0.161 * \varphi) + 0.198 * sin(0.1601 * \varphi) \quad \text{Rolling} \quad (16d)$$
$$Cy = 0.1314 - 0.0753 * cos(0.0564 * \varphi) + 0.1323 * sin(0.0564 * \varphi) \quad \text{Yawing} \quad (16e)$$
$$Cp = 0.0952 * sin(0.0385 * \varphi + 3.009) \quad \text{Pitching} \quad (16f)$$

Figure 21 shows the force coefficients of the sedan against the yaw angle and the fitting curve based on these coefficients. It can be seen that the fitted curve lines using the equations proposed in this paper agree well with the simulation results.

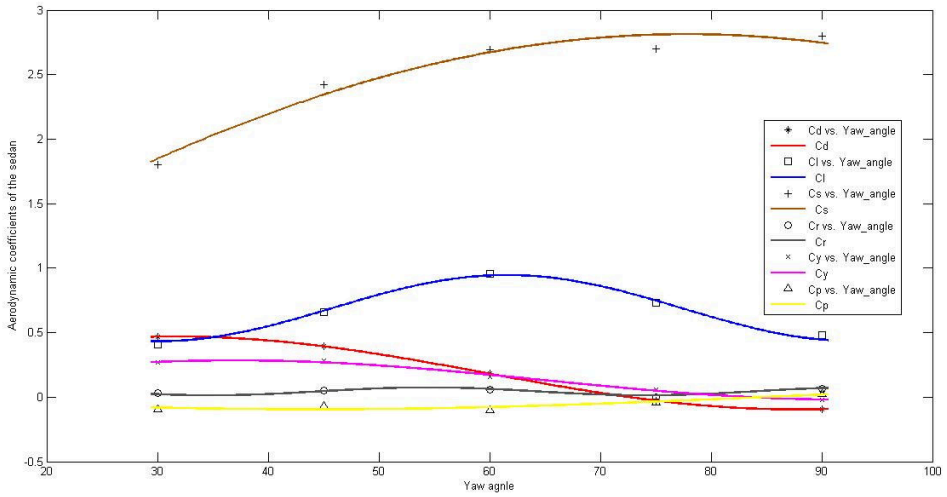

Figure 21 Aerodynamic coefficients against yaw angle

4.2 Results of the simulator tests

4.2.1 Time history of the vehicle performance

In this study, the vehicle's performance was recorded as lane offset (a), steering angle (δ) and vehicle velocity (V_v) as shown in Figures 22-27. The vehicle lane offset, steer angle and vehicle velocity in dry day under wind type 2 are drawn as Figures 22, 24, and 26. These variables of the vehicle under wind type 2 in rainy weather are exhibited in Figures 23, 25, and 27. These figures and Table 6 together reflect that the harsh weather environment influences the vehicle performance apparently.

The directions of lane offset are corresponding to the wind directions in dry weather as well as in rainy weather. For an example, when the crosswind blew from vehicle's right side to the left side, the vehicle trajectory off occurs on the left side of the longitudinal central line of the vehicle. It can be seen from Figures 23 and 24 that the steering angle has the same trend with the crosswind in both dry day and rainy weather, which means the same direction and similar

pattern. However, the same trend does not match the concept that the driver tried to correct the course deviation and adjust the steering wheel against the crosswind. The explanation of this conflict is that the wind loads were applied on the vehicle through the changes of feeling and vision. When the wind blowing on the vehicle, the steering wheel changes an angle in accordance with the wind forces, making the driver feeling "lose control" as well as the view angle changes a little. The vehicle's velocity perpendicular with crosswind in windy dry weather and windy rainy weather is shown in Figures 26 and 27; the variation of the vehicle's velocity is fairly constant with the time lapses in both inclement weather conditions.

For the wind type 2, the mean value of three variables, lane offset (a) and recorded steering angle (δ) were also investigated. In Figure 28, the mean value of the vehicle lane offsets in both strong windy weather and windy rainy weather are drafted. It is clear that the larger crosswind speed causes a larger lane offset and a smaller wind speed causes a smaller one. In Figure 29, the mean steering angle in both windy weather and windy rainy weather are displayed. There is an obvious correction angle right after when wind is acting on the vehicle. The mean vehicle velocity (V_v) has a same trend in both windy dry day and windy rainy day, and the two mean values are around 32 m/s according to the Figure 30. Though mean-value curves for the three variables in different weather conditions depict very similar vehicle performance, the statistic study is conducted to determine the influence of such factors, including the weather and the driving time.

Table 6 demonstrates the Analysis of variance (ANOVA) results of the vehicle variables utilizing MATLAB, and the significance level (alpha) is selected as 0.001 to be sure that any significant difference in the vehicle performance does exist. The environment effects means the wind and rain affecting separately, and the wind and rain work together. On the other hand, the statistic investigation of the different day aims on the repeatability of the vehicle performance and driver behavior, which requires the driver taking the test in different times. Thus, researchers repeated the experiments in different discontinuous days spanning a month. From the Table 6, the harsh environments and different days influence the vehicle's land offset (P-value<0.0001), steering angle (P-value<0.0001), and vehicle velocity (P-value<0.0001), respectively. In other words, these variables defined for vehicle performance are obtained without repletion and the vehicle performance is significantly different among drive time and driving environments.

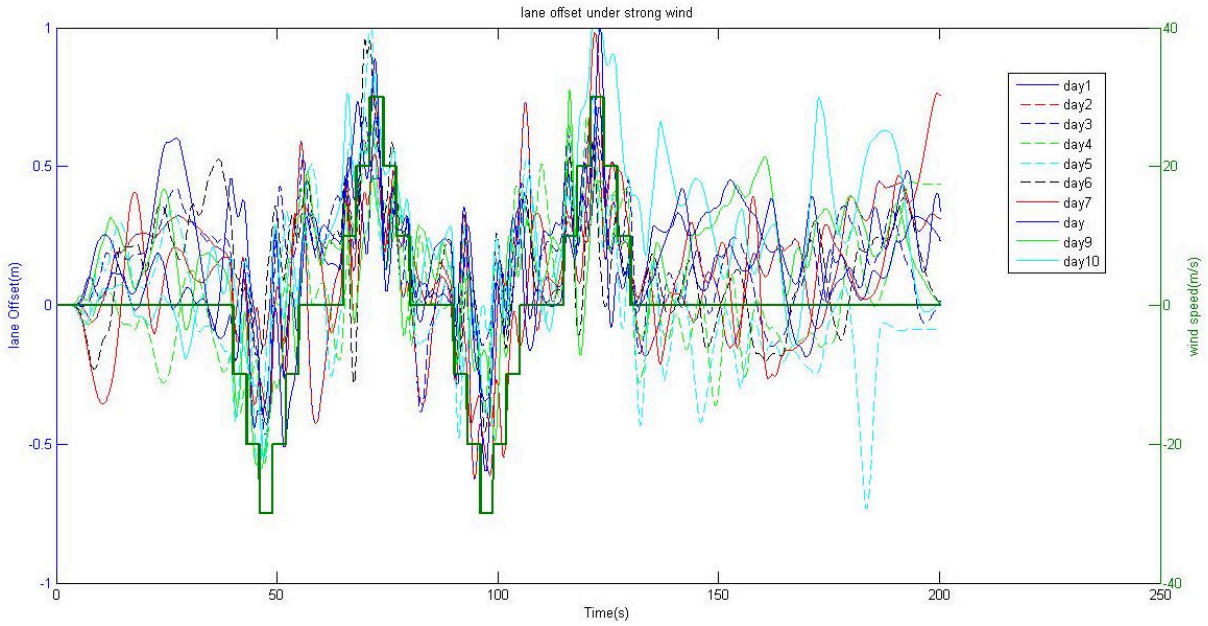

Figure 22 Lane offset in dry day

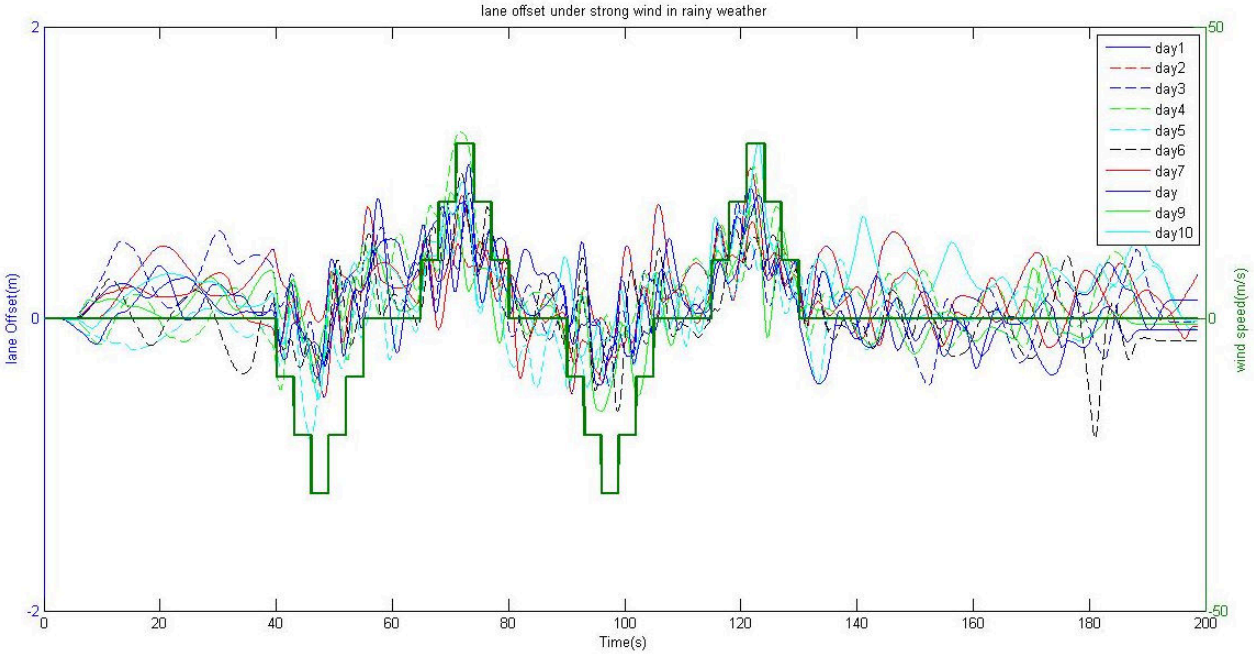

Figure 23 Lane offset in rainy weather

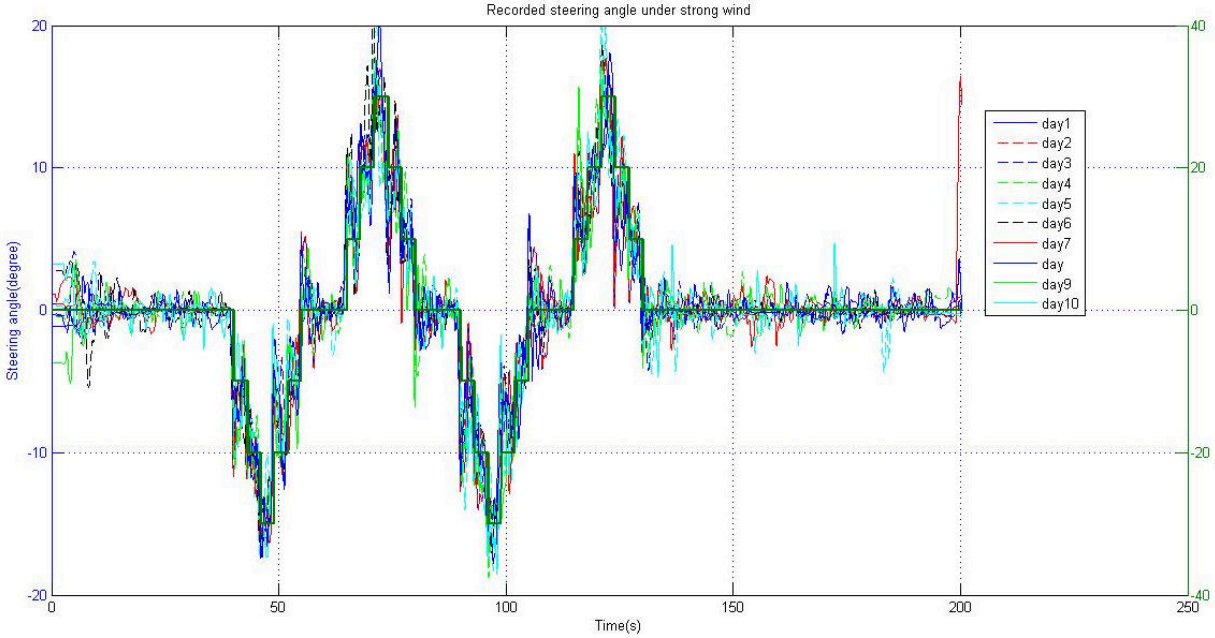

Figure 24 Recorded steering angle in dry

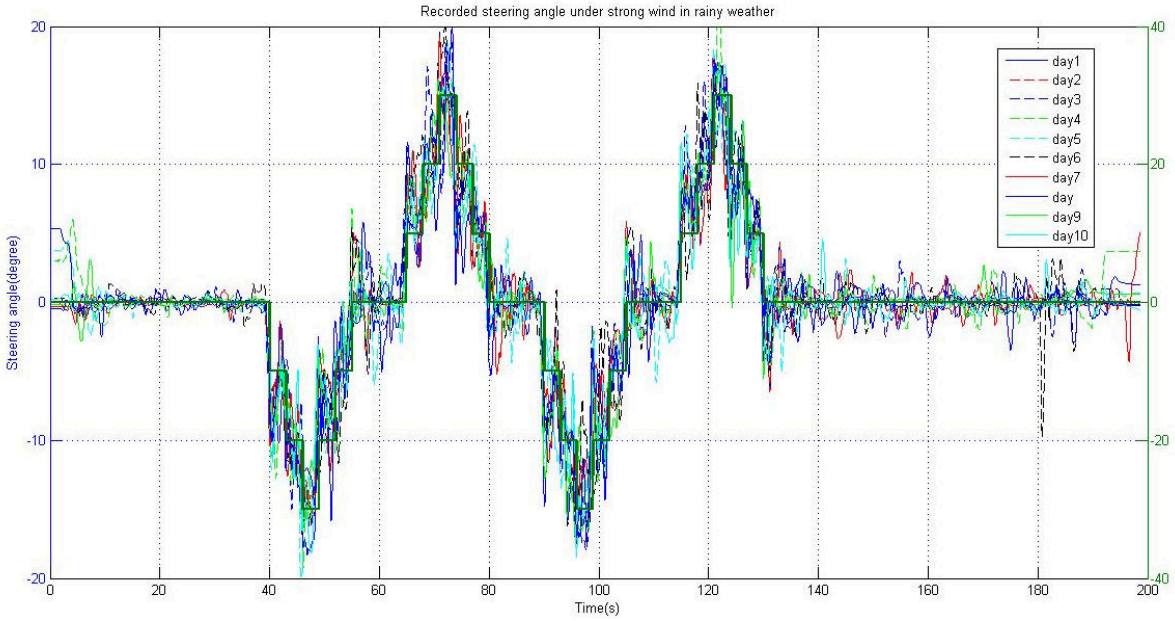

Figure 25 Recorded steering angle in rainy weather

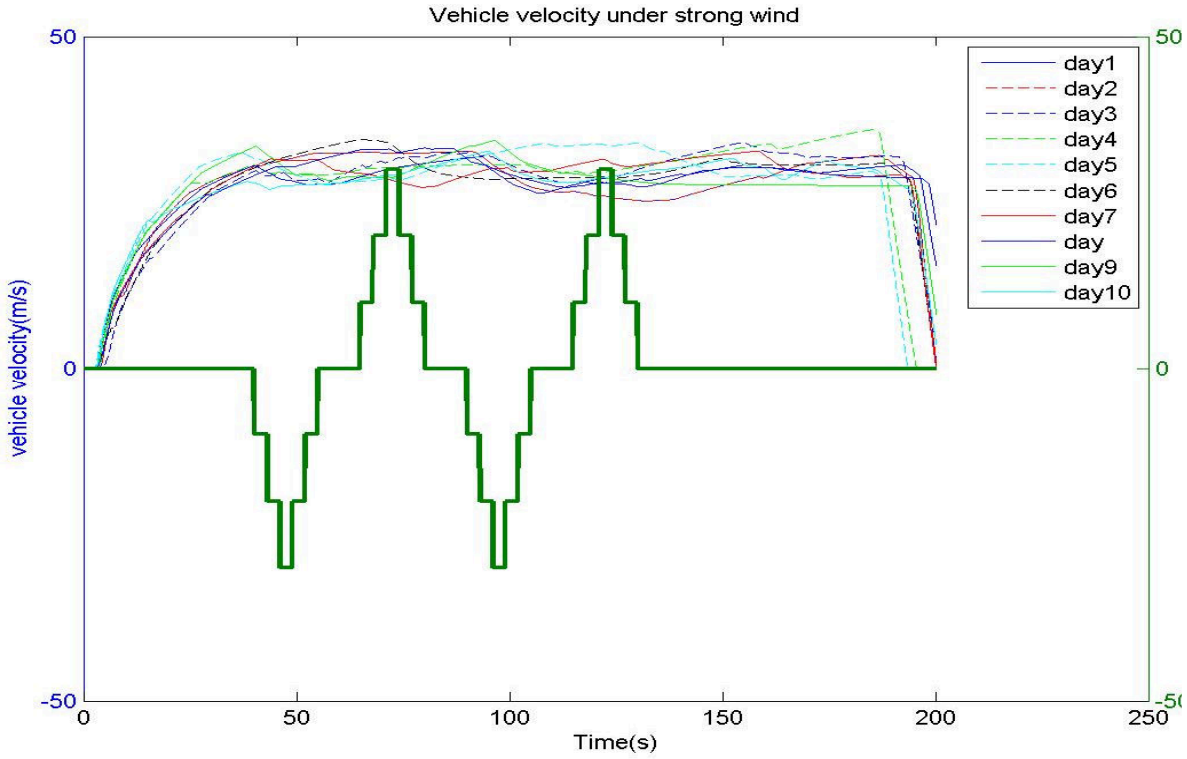

Figure 26 Vehicle velocity in dry day

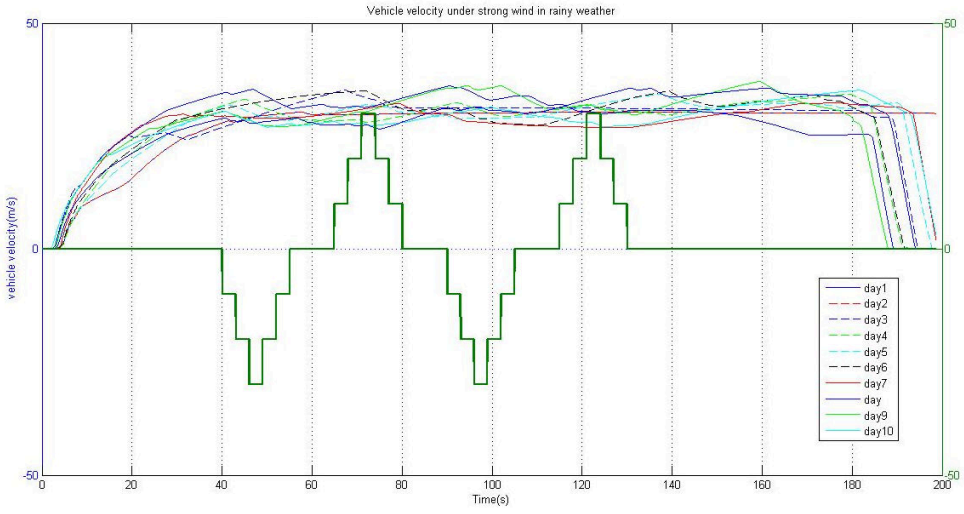

Figure 27 Vehicle velocity in rainy weather

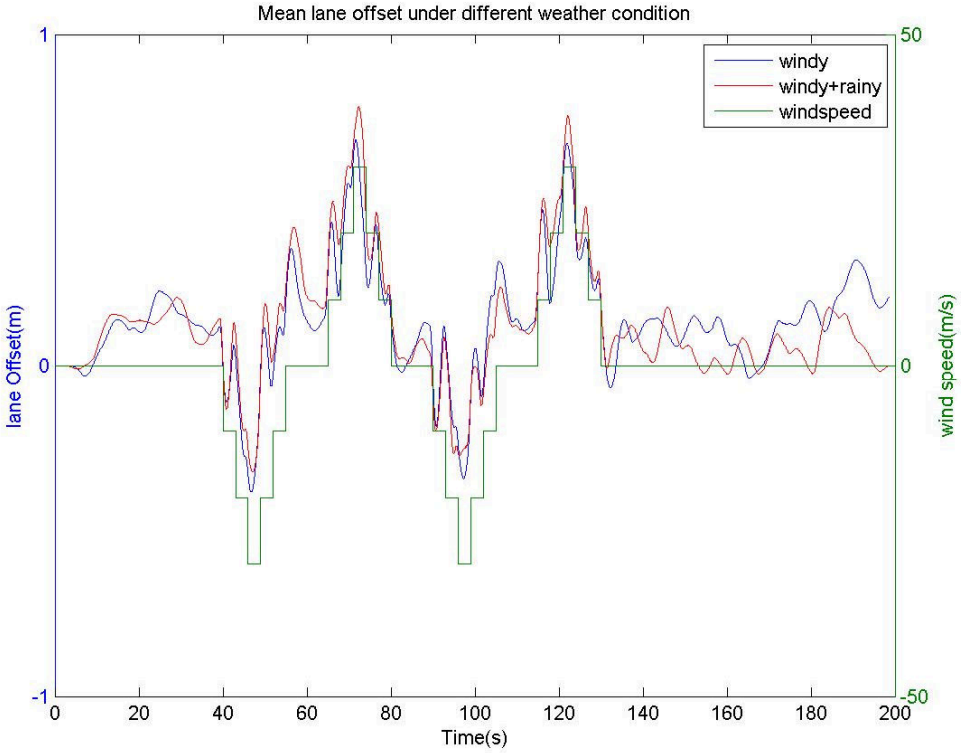

Figure 28 Mean lane offset of the vehicle under different weather conditions

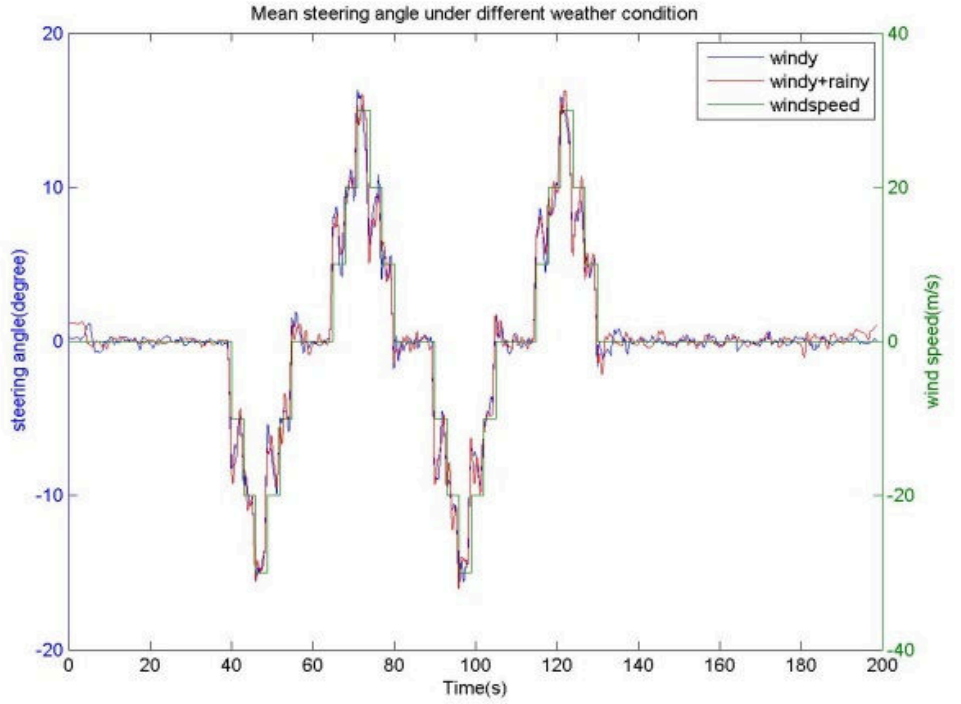

Figure 29 Means steering angle of the vehicle under different weather conditions

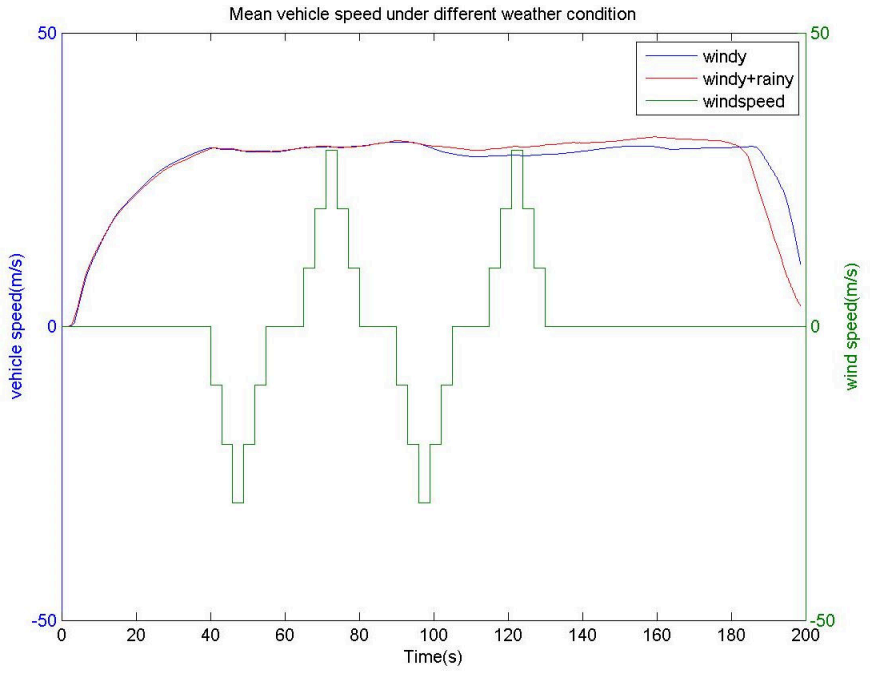

Figure 30 Means vehicle velocity under different weather conditions

Table 6 Segmental ANOVA results of selected variables

Road off (a)					
Effect	SS	DF	MS	F	Prob>F
Harsh environments	61.5817	3	20.5272	8039.65	<0.0001
Different days	120.66	9	13.4072	776.5	<0.0001
Steering angle (δ)					
Harsh environments	85301.8	3	28433.9	90354.6	<0.0001
Different days	536	9	59.4438	10.63	<0.0001
Vehicle velocity (V_v)					
Harsh environments	10023.3	3	3341.11	58559.73	<0.0001
Different days	2167.78	9	240.865	1166.33	<0.0001

The impacts of the rain weather excluding the strong wind on the vehicle performance are investigated, and partial statistic results of the three selected variables are listed in Table 7. Through comparison between the mean value curves of the vehicle lane off under the two road surface conditions, a conclusion can be made that the mean value of the lane offset in windy dry weather has little difference with the one of windy rainy weather in most time point, which is supported by statistic results as well (P-value=0.0024>0.001). In other words, a variation of tire frictions does not affect the mean lane off substantially in non-windy weather, which may be induced by the raining volume and the number limit of tire frictions tested in the experiments. Similar conclusions are made as well as the steer angle and the vehicle velocity. However, the

rain does affect the vehicle lane off and steering angle if choosing the significance level with 0.05 while the vehicle velocity is insignificant influenced by the rain.

Table 7 Statistic results of the effect of road surface conditions

Effect	Variables	SS	DF	F	Prob>F
Road surface condition (dry VS wet, no wind)	a	0.01299	1	9.24	0.0024
	δ	0.3373	1	7.11	0.0078
	V_v	10.7	1	1.73	0.1888

4.2.2 Lateral displacement (Δ) due to the wind

Similar to section 4.2.1, the lateral displacements of the vehicle induced by the strong wind in dry weather and in rainy weather were obtained. Table 8 shows the lateral displacement of the vehicle when subjected to crosswinds. The rainy weather affected the vehicle's performance inconspicuously (P-value>0.001). Under both drivers' operations, the mean lateral displacements of the vehicle were larger than that of the vehicle in dry day. The difference of tire frictions on dry road surfaces and on wet road surfaces induced the difference of the mean lateral displacement of the vehicle. In the dry day under strong wind, the mean value of the lateral displacement of driver 2 was smaller than that of driver 1, which may be because the first hitting wind speed was 10 m/s for the driver 2 while 30 m/s for driver 1 (i.e., they are under two different wind conditions). Therefore, the higher wind speed suddenly attacks the vehicle, and the larger lateral displacement occurred.

Table 8 The lateral displacement of vehicle at wind first hitting (unit: m)

	Driver 1		Driver 2	
	Windy	Windy + Rainy	Windy	Windy + Rainy
Day 1	1.209	1.5095	0.0474	0.1834
Day 2	1.3977	1.5980	0.1437	0.1438
Day 3	0.5879	0.8560	0.1313	0.4253
Day 4	0.9571	1.2197	0.1135	0.2613
Day 5	1.1265	1.4685	0.1544	0.1496
Day 6	0.8362	1.1626	0.1554	0.1676
Day 7	0.8129	0.7436	0.0671	0.2208
Day 8	1.2680	1.6270	0.2269	0.0601
Day 9	0.8667	1.0960	0.3066	0.1153
Day 10	0.6476	0.8867	0.1277	0.1022
Mean lateral displacement (Δ)	0.8593	1.2168	0.1475	0.1829
Standard deviation	0.2948	0.3237	0.0746	0.1029
F	3.4		0.43	
P-value	0.0819		0.5205	

4.2.3 Vehicle sideslip time due to the wind

In general, when subjected to crosswind, vehicles may avoid traffic crash in a medium traffic flow if the sideslip time and lateral displacement is appropriately small. With a function of reflecting the crash risk of a vulnerable vehicle driving through inclement weather, the vehicle sideslip time due to the wind first hitting is critical as well as the lateral displacement caused by the strong wind. Similar to the lateral displacement, sideslip time is also investigated and listed in Table 9. The weather factors have different impact on the sideslip time. For example, the rain induces different sideslip time significantly (P-value<0.0001) when driver 1 take the tests while the driver 2 plays insignificant (P-value =0.7839) difference in the two inclement weathers. These may be caused by the driver's driving experiences in harsh environments. That is, driver 2 has more experience driving in windy rainy weather than driver 1, so driver 2 can handle the vehicle in windy rainy condition as well as in only windy condition.

Table 9 The vehicle sideslip time of vehicle at wind's first hitting (unit: s)

	Driver 1		Driver 2	
	Windy	Windy + Rainy	Windy	Windy + Rainy
Day 1	2.2914	2.0645	1.4150	4.0167
Day 2	2.8253	2.198	2.0816	1.7311
Day 3	2.5583	1.9143	2.0150	1.7311
Day 4	2.7752	1.9143	1.6650	1.6977
Day 5	2.9421	2.0311	3.2316	4.0167
Day 6	2.5083	1.7308	2.0317	1.3974
Day 7	2.4916	1.7642	1.6483	2.4652
Day 8	2.7919	2.3481	2.0150	2.1148
Day 9	2.4749	2.2313	4.0149	2.0981
Day 10	2.2747	2.0144	4.0149	1.6644
Mean reaction time	2.5934	2.0211	2.4134	2.2933
Standard deviation	0.2293	0.1993	0.9737	0.9560
F	35.47		0.08	
P-value	<0.0001		0.7839	

4.2.4 Driver's reaction time

As defined in section 3.2.5, the driver's reaction time reflects the delay time between the starting time of wind speed and the starting time when the driver compensates the course deviation. There are many factors impacting the driver's reaction time. For instance, the density of the rain falling on the vehicle impacts the vision of the drivers; in other words, heavy rain may

weaken the drivers' view sight when driving and vice versa. The reaction time also depends on the driver's health and mental conditions as well as the external environments.

Table 10 shows the reaction times of driver 1 who took the test under wind type 1 and driver 2 who took the test under wind type 2. In the ten tests days, drivers react to the strong wind in less than 1 second in both dry days and rainy days as shown in Table 10. The average reaction times for both two drivers are 0.7 s in both inclement weather conditions. In addition, there is no serious evidence to conclude that the rain has a significantly effect on the two drivers' reaction time (P-value>0.0001), which may be caused by the low density of rain falling.

Table 10 Reaction time of each driver (unit: s)

	Driver 1		Driver 2	
	Windy	Windy + Rainy	Windy	Windy + Rainy
Day 1	0.7646	0.5984	0.5650	0.6150
Day 2	0.6146	0.74840	0.6317	0.8517
Day 3	0.6980	1.3480	0.7484	0.5984
Day 4	0.5813	0.6650	0.5817	0.6317
Day 5	0.6646	0.7317	0.5317	0.5317
Day 6	0.6980	0.6484	0.6484	0.5984
Day 7	0.6313	0.5817	0.6817	0.8650
Day 8	0.6480	1.0817	0.7817	0.5650
Day 9	0.6646	0.5984	0.6650	0.8650
Day 10	0.6146	0.8150	0.6984	0.6984
Mean reaction time	0.6580	0.7817	0.6534	0.6820
Standard deviation	0.0528	0.2481	0.0794	0.1305
F	2.38		0.36	
P-value	0.1404		0.5604	

5. SUMMARY AND CONCLUSIONS

With the economic booming development of coastal areas, the importance of traffic planning becomes obvious not only in the case of hurricane evacuations but also in daily transportation. Vehicle performance on the freeway during harsh environments is critical to the success of the planning process. On the other hand, large trucks are vulnerable under strong wind due to the large wind forces caused by their large size shapes. Adverse driving environments and roadway conditions have been blamed for single vehicle accidents, and a series of bad collisions resulted from roadway offset and large heading error. Vehicle safety not only threatens people's lives during normal operations, but also may even put many people in miserable situations when an emergency evacuation is interrupted by accidents on key routes. As a result, the safety of many people who are stuck in the evacuation routes may be jeopardized. The causes of single-vehicle accidents can be very complicated: from a single primary reason such as a strong gust to the combination of several reasons such as weather conditions, vehicle conditions, road surface conditions, driver operational errors, etc. Thus, it is important to understand the performance of vehicle and driver behavior in hazardous driving environments.

The present study is carried out with a goal of replicating the natural environments and investigating the safety of vehicles under normal operations in harsh weather conditions. An attempt has been made to obtain numerically the wind forces of the vehicle and simulate the inclement weather, road surface, and driver operational process with a driving simulator.

Aiming on the investigation of the vehicle performance and the driver's reaction when driving through strong crosswind areas, the authors have studied the wind forces acting on the moving vehicle by the computational fluid dynamic (CFD) method and conducted driving simulator tests using the driving simulator installed in Louisiana State University. Firstly, a sedan type vehicle was chosen as the discussing vehicle type and its parameters, such as geometry dimensions and weight, were also studied. Secondly, the numerical simulations of the flow field around the vehicle were carried out and the wind forces on the vehicle were predicted. Finally, the LSU driving simulator was used to investigate the driver's behavior and vehicle performance in different adverse conditions such as strong crosswinds and wet road surface. After obtaining the vehicle wind forces, two drivers were recruited for two different wind type conditions and each driver took tests for ten days in which he/she drove in assigned scenario for one time every day.

Based on the results of the numerical simulations, wind forces on the sedan were determined as well as the vehicle performance and the driver's behavior. The following are some highlights from the discussion conducted in this study.

- Numerical simulation using the CFD method is an efficient way of investigating wind forces/aerodynamic coefficients of vehicles. In addition, sliding mesh technology is a good choice to help simulate the relative motion between the vehicle and the road surface.
- Vehicle's motion affects the aerodynamic coefficients of the vehicle, and the aerodynamic coefficients can be expressed as functions of the yaw angle between the vehicle direction and the wind direction.
- The simulator can model different weather scenarios including strong crosswinds and rainy weather, in which the wind forces on the vehicle are the real time wind effects associated with the vehicle velocity and the wind velocity.
- A higher wind speed leads to a larger mean lateral displacement when crosswinds first hit the vehicle as well as a larger lane offset during the crosswinds attacking time.
- The vehicle's performance such as lane offset, steering angle, and vehicle velocity are significantly different (P-value<0.0001) between driving environments and driving days.
- Vehicle displays no obvious different (P-value>0.0001) performance on dry road surface and wet road surface excluding the wind action in this study.
- Drivers' reaction times are insignificantly influenced by the rain falling.

The present study has demonstrated a feasible approach to study the driver and vehicle behavior, which, through a future more comprehensive study, may provide a useful basis for traffic designs on highways with complicated topographic and weather conditions and optimization of evacuation routes and strategy that may in turn lead to minimized single-vehicle crash risks.

6. FUTURE WORKS AND RECOMMENDATIONS

In this study, there was only one vehicle type studied both in the numerical aerodynamic simulation and the driving simulator tests, which is far less than the vehicle types of daily transportation. Thus, more vehicle types, such as SUV's, bus', and tractor-trailer's should be studied in future works. On the other hand, the adverse weather, road surface, such as snow, traffic flow and different vehicle types can also be studied in order to replicate the natural driving environments. Finally, the steering processes of the driver and acceleration/deceleration of the vehicle can be observed as the driver behavior and the vehicle performance.

A further vehicle safety assessment method could turn to the numerical study through developing a comprehensive and systematic accident model and introducing accident critical variables to predict and prevent the accident risks under hazardous driving condition. The numerical model obtains the vehicle's accident-related response in different environments, and the accident risks can be assessed in real-time. Based on the outputs of the accident model, traffic designers could optimize the transportation with low single-vehicle accident risks, and road management companies can make proper strategies for the evacuation routes in extreme weather conditions.

7. REFERENCES

Angelis, W., Drikakis, D., Durst, F. and Khier, W. (1996), "Numerical and experimental study of the flow over a two-dimensional car model", J. Wind Eng. Ind. Aerodyn. 62, 57-79.

Baker, C. J. (1986a), "A simplified analysis of various types of wind-induced road vehicle accidents", J. Wind Eng. Ind. Aerodyn., 22, 69-85.

Baker, C.J. (1986b), "Train aerodynamic forces and moment from moving model experiments", J. Wind Eng. Ind. Aerodyn., 24, 227-251.

Baker, C.J. (1987), "Measures to control vehicle movement at exposed sites during windy periods", J. Wind Eng. Ind. Aerodyn., 25, 151-161.Baker, C. J. (1991a), "Ground vehicles in high cross winds .1. Steady aerodynamic forces", J. Fluid Struct., 5, 69-90.

Baker, C. J. (1991b), "Ground vehicles in high cross winds .2. Unsteady aerodynamic forces", J. Fluid Struct., 5, 91-111.

Baker, C. J. (1991c), "Ground vehicles in high cross winds .3. The interaction of aerodynamic forces and the vehicle system", J. Fluid Struct., 5, 221-241.

Baker, C. J. (1994), "The quantification of accident risk for road vehicles in cross winds", J. Wind Eng. Ind. Aerodyn., 52, 93-107.

Bettle, J., Holloway, A.G.L., and Venart, J.E.S. (2003), "A computational study of the aerodynamic forces acting on a tractor-trailer vehicle on a bridge in cross-wind", J. Wind Eng. Ind. Aerodyn., 91, 573-592.

Cairns, R.S. (1994), "Lateral aerodynamic characteristics of motor vehicles in transient crosswinds", Ph.D. dissertation, Cranfield University, Cranfield.

Cejun Liu, and Rajesh Subramanian. "Factors related to fatal single-vehicle run-off-road crashes" National Highway Traffic Safety Administration.

Cheli, F., Ripamonti, F., Rocchi, D. and Tomasini, G. (2010), "Aerodynamic behavior investigation of the new EMUV250 train to cross wind", J. Wind Eng. Ind. Aerodyn., 98, 1889-201.

Cheli, F., Corradi, R., Sabbioni, E. and Tomasini, G. (2011a), "Wind tunnel tests on heavy road vehicles: Cross wind induced loads-Part2", J. Wind Eng. Ind. Aerodyn., 99, 1011-1024.

Cheli, F., Corradi, R., Sabbioni, E. and Tomasini, G. (2011b), "Wind tunnel tests on heavy road vehicles: Cross wind induced loads-Part1", J. Wind Eng. Ind. Aerodyn., 99, 1000-1010.

Coleman, S.A., and Baker, C.J. (1990), "High sided road vehicles in cross winds", J. Wind Eng. Ind. Aerodyn., 36, 1383-1392.

Corin, R.J., He, L. and Dominy, R.G. (2008), "A CFD investigation into the transient aerodynamic forces on overtaking road vehicle models", J. Wind Eng. Ind. Aerodyn., 96, 1390-1411.

Corsello, Patricia. (1993). "Evaluation of surface friction guidelines for Washington state highways". Washington State Transportation Center.

Favre, T. (2011), "Aerodynamics simulations of ground vehicles in unsteady crosswind", Ph.D. dissertation, KTH School of Engineering Sciences, Stockholm.

Federal Highway Administration. (2013). http://ops.fhwa.dot.gov/weather/q1_roadimpact.htm.

Fluent Inc. (2011), FLUENT Theory Guide, Fluent Inc.

Guilmineau, E. (2008), "Computational study of flow around a simplified car body", J. Wind Eng. Ind. Aerodyn., 96, 1207-1217.

Guilmineau, E., Chikhaoui, O., Deng, G.B. and Visonneau, M. (2013), "Cross wind effects on a simplified car model by a DES approach", Comput. Fluids, 78, 29-40.

Guiney, John L. and Lawrence, Miles B. (1999). "Hurricane Mitch Preliminary Report". National Hurricane Center.

Gunther, E. B., Cross, R. L., and Wagoner, R. A. (1983). "Eastern North Pacific Tropical Cyclones of 1982". Monthly Weather Review, 111(5), 1080-1102.

Hall, J.W., L.T. Glover, K.L. Smith, L.D. Evans, J.C. Wambold, T.J. Yager, and Z. Rado, (2006), "Guide for Pavement Friction". Project No. 1-43, Final Guide, National Cooperative Highway Research Program, TRB, Washington D.C.

Han, Y., Hu, J.X., Cai, C.S., Chen, Z.Q. and Li, C.X. (2013), "Experimental and numerical studies of aerodynamic forces on vehicles and bridges", Wind Struct., 17(2), 163-184.

Henry, J. J. (2000). "Highway Capacity Manual 2000 Evaluation of Pavement Friction Characteristics". NCHRP Synthesis 291, TRB, National Research Council, Washington, D.C.

Holland, G. J. (1993). Global Guide to Tropical Cyclone Forecasting. http://cawcr.gov.au/bmrc/pubs/tcguide/ch9/ggch9.htm

Holmes, J. D. (2001), Wind loading of structures, Spon Press, Abingdon, UK.

Hucho, W.H. (1993), "Aerodynamics of road vehicles", Annu. Rev. Fluid Mech., 25, 485-537.

Humphreys, N.D. and Baker, C.J. (1992), "Forces on vehicles in cross winds from moving model tests", J. Wind Eng. Ind. Aerodyn., 41-44, 2673-2684.

Ibrahim, A.T., and F.L. Hall. (1994). Effect of Adverse Weather Conditions on Speed-Flow-Occupancy Relationships, Transportation Research Record 1457, Transportation Research Board, Washington, D.C.

Ishak, S., Codjoe, J., Rodriguez, J., Thapa, R., Russell, M., Osama, O., and Jenkins, S. (2013). Moldeling the effect of gusty hurricane wind force on vehicles using LSU driving simulator. Louisiana Department of Transportation and Development.

Ju sam oh, Yong Un shim, and Yoon Ho Cho (2002), "Effect of weather conditions to traffic flow on freeway" KSCE Journal of Civil Engineering, Vol. 6, No. 4, 413-420.

Keerthana, M., Jaya, K.P., Rajan, S.S., Thampi, H. and Sankar, R.R. (2011), "Numerical studies on evaluation of aerodynamic force coefficients of cable-stayed bridge deck", J.Wind Eng., 8(2), 19-29.

Knabb, R. D., Rhome, J. R. and Brown, D. P., (2005), Tropical Cyclone Report Hurricane Katrina: August 23-30, National Hurricane Center.

Krajnovic,S. and Davidson, L. (2002), "Large eddy simulation of the flow around a bluff body", AIAA J., 40(5), 927-936.

Krajnovic, S. and Davidson, L. (2003), "Numerical study of the flow around the bus-shaped body", J. Fluids Eng. ASME, 125, 500-509.

Krajnovic, S. and Davidson, L. (2005a), "Influence of floor motions in wind tunnels on the aerodynamics of road vehicle", J. Wind Eng. Ind. Aerodyn., 93, 677-696.

Krajnovic, S. and Davidson, L. (2005b), "Flow around a simplified car, Part1: large eddy simulation", J. Fluids Eng. ASME, 127,907-918.

Krajnovic, S. and Davidson, L. (2005c), "Flow around a simplified car, Part2: understanding the flow", J. Fluids Eng. ASME, 127, 919-928.

Krajnovic, S., Bengtsson, A. and Basara, B. (2011), "Large eddy simulation investigation of the hysteresis effects in the flow around an oscillating ground vehicle", J. Fluids Eng. ASME, 133(12), 121103.

Krajnovic, S., Ringqvist, P., Nakade, K. and Basara, B. (2012), "Large eddy simulation of the flow around a simplified train moving through a crosswind flow", J. Wind Eng. Ind. Aerodyn., 110, 86-99.

Kyte, M, Khatib, Z, Shanon, P., and Kitchener, F. (2001). "Effect of Weather on Free-Flow Speed" Transportation Research Record, vol. 1776, 61-68,.

Malviya, V., Mishra, R. and Fieldhous J. (2009), "CFD investigation of a novel fuel-saving device for articulated tractor-trailer combinations", Eng. Appl. Comput. Fluid Mech., 3(4), 587-607.

NHTSA. (2008). "Naional motor vehicle crash causation survey report to congress", National Highway Traffic Safety Administration, DOT-HS-811-059, 2008.

NOAA, National Weather Service . (2008). Weather Term Definitions. Retrieved 10/03/2015, from http://pajk.arh.noaa.gov/wxWords/wxWords.php?alpha=G

NOAA, National Weather Service. (2011). The Enhanced Fujita Scale (EF Scale). Retrieved 10/03/2015 , from http://www.spc.noaa.gov/efscale/

NOAA, National Weather Service. (2012). Tropical Cyclone Climatology. Retrieved 10/03/2015, from http://www.nhc.noaa.gov/climo/

NOAA. National Weather Service. (2013). Glossary of NHC Terms. Retrieved 10/03/2015, from http://www.nhc.noaa.gov/aboutgloss.shtml

Osth, J. and Krajnovic, S. (2012), "The flow around a simplified tractor-trailer model studied by large eddy simulation", J. Wind Eng. Ind. Aerodyn., 102, 36-47.

Osth, J. and Krajnovic, S. (2014), "A study of the aerodynamics of a generic container freight wagon using Large-Eddy Simulation", J. Fluid Struct., 44, 31-51.

Pacejka, H.B., (2006), Tire and Vehicle Dynamics, Butterworth-Heinemann, 2nd edition.

Patten, J. McAuliffe, B. Mayda, W. and Tanguay, B. (2012), "Review of aerodynamic drag reduction devices for heavy trucks and buses", Technical report, NRC-CNRC.

Pielke, Jr., R. A., Gratz, J., Landsea, C. W., Collins, D., Saunders, M. A., and Musulin, R. (2008). Normalized Hurricane Damages in the United States: 1900-2005. Natural Hazards Review, 9(1), 29-42.

Powell, Mark D., Houston, Samuel H., & Reinhold, Timothy A. (1996). "Hurricane Andrew's Landfall in South Florida. Part I: Standardizing Measurements for Documentation of Surface Wind Fields". Weather and Forecasting, 11(3), 304-328.

Reynolds, Osborne. (1895). "On the Dynamical Theory of Incompressible Viscous Fluids and the Determination of the Criterion." Philosophical Transactions of the Royal Society of London. A. 186, 123-164.

Robert Bosch GmbH. (1996) Automotive Handbook. 4th ed., Robert Bosch GmbH.

Rodriguez, Jose M. (2014). Modeling the effect of Gusty Hurricane wind force on vehicles using the LSU driving simulator. Master thesis, Louisiana State University.

Sanchez, Ray. CNN(2015). Hurricane Patricia dissipates in Mexico; flooding, mudslide concerns remain. Retrieved 11/03/2015. http://www.cnn.com/2015/10/24/americas/hurricane-patricia/

Simiu, E. and Scanlan, R. H. (1996), Wind effects on structures-Fundamentals and Applications to Design, 3rd edition, John Wiley & Sons Publication, Hoboken, NJ, USA.

Shirai, S. and Ueda, T. (2003), "Aerodynamic simulation by CFD on flat box girder of super-long-span suspension bridge", J. Wind Eng. Ind. Aerodyn., 91, 279-290.

Stull, R. B. (1988). An introduction to Boundary Layer Meteorology: Kluwer Academic.

Stull, R. B. (1995). Meteorology Today for Scientist and Engineers: West Publishing Co.

United States. Department of Commerce. National, Oceanic, Atmospheric Administration. National Weather, Service, United States. Department of Homeland Security. Federal Emergency Management, Agency, & American Red, Cross. (2012). Tropical cyclones : a preparedness guide. [Silver Spring, Md.]: U.S. Dept. of Commerce, National Oceanic and Atmospheric Administration, National Weather Service.

USDOT. (2015). "Large truck and bus crash facts 2013." Federal Motor Safety Administration, U.S. Dept. of Transportation, Washington, D.C.

Wang, B., Xu, Y.L., Zhu, L.D., Cao, S.Y. and Li, Y.L. (2013), "Determination of aerodynamic forces on stationary/moving vehicle-bridge deck system under crosswind using computational fluid dynamics", Eng. Appl. Comput. Fluid Mech., 7(3), 355-368.

Wang, Hao, Imad L. Al-Qadi, Ilinca Stanciulescu, (2010). "Effect of Friciton on Rolling Tire – Pavement Interaction" USDOT Region V Regional University Transportation Center Final Report.

Weyman, J. C., and Anderson-Berry, L. J. (2008). Societal Impacts of Tropical Cyclones. http://www.aoml.noaa.gov/hrd/iwtc/AndersonBerry5-1.html